8. ASAC JunganalytikerInnen Forum

01. Juni (13:30) – 02. Juni (16:45) 2012

an der Naturwissenschaftlichen Fakultät der Paris-Lodron-Universität Salzburg

Programm
&
Book of Abstracts

Photonachweis: Universität Salzburg

Sponsoren des Meetings

Agilent Technologies

AB SCIEX

BRUKER

PerkinElmer® For the Better

Werfen Group | Instrumentation Laboratory

Metrohm INULA GmbH

SHIMADZU Excellence in Science

Thermo SCIENTIFIC Part of Thermo Fisher Scientific

phenomenex® ...breaking with tradition℠

VWR®

WILEY

8. ASAC JunganalytikerInnen Forum 01.06. – 02.06.2012

Programm

Freitag, 01.06.2012

ab 12:45: **Registrierung an der Naturwissenschaftlichen Fakultät (Erdgeschoß) im Foyer vor dem HS 403 (Grüner Hörsaal)**

13:30 Begrüßung und Eröffnung durch den Präsidenten der ASAC Herrn Wolfgang Buchberger und Herrn Hanno Stutz; Präsentation der Sponsoren

Chair: Hanno Stutz

13:45 **Key Lecture**
Testing in analytical chemistry – pitfalls, and how to reduce them
Michael Bickel, Institute for Reference Materials and Measurements (IRMM), Joint Research Centre (JRC), European Commission, Geel, Belgium

Session 1: Quality control, uncertainty budgets, validation

Chair: Herbert Oberacher & Silke Ruzek

14:15 **O1:** Phosphorothioate Oligonucleotide Characterization by Micro Liquid Chromatography - Mass Spectrometry
Robert Erb, Institute of Legal Medicine, Innsbruck Medical University, Innsbruck

14:35 **O2:** Comparison of different MS platforms for determination of mass isotopomer distribution in cellular samples
Raffaele Guerrasio, Austrian Centre of Industrial Biotechnology (ACIB), University of Natural Resources and Life Sciences – Division of Analytical Chemistry, Department of Chemistry, BOKU Vienna , Vienna

15:05 **O3:** Quality control of human rhinovirus serotype 2 preparations by orthogonal analysis methods
Victor U. Weiss, Institute for Chemical Technologies and Analytics, Vienna University of Technology, Vienna

15:25-15:50 **Kaffeepause im Foyer**

Session 2: Capillary electrophoresis (CE), CE-MS, ICP-MS

Chair: Christian Klampfl & Lisa Fischer

15:50 **O4:** Application of capillary isoelectric focusing (CIEF) for the characterization of proteins/allergens
Theresa Kristl, Division of Chemistry and Bioanalytics, Department of Molecular Biology, University of Salzburg, Salzburg

16:10 **O5:** Characterization of nitrated allergens by various capillary electrophoresis modes
Sergey Gusenkov, Division of Chemistry and Bioanalytics, Department of Molecular Biology, University of Salzburg, Salzburg

16:30 **O6:** CE and CE-ESI-MS studies to elucidate the hydrolysis behavior of anticancer bis(acetoxime)-dihalidoplatinum(II) complexes
Gerlinde Grabmann, Institute of Inorganic Chemistry, University of Vienna, Vienna

16:50 **O7:** Quantitative determination of cisplatin-protein interaction in cell models by LC-ICP-MS
Gerrit Hermann, Division of Analytical Chemistry, Department of Chemistry, University of Natural Resources and Life Sciences, Vienna

17:10-17:30 **Kaffeepause im Foyer**

Session 3: Phosphoproteins/-peptides; AFM
Chair: Christian Huber & Evelyn Rampler

17:30 **O8:** Highly selective isolation of phosphoproteins using trivalent lanthanide-ion precipitation
Yüksel Güzel, Institute of Analytical Chemistry and Radiochemistry, Leopold-Franzens University, Innsbruck

17:50 **O9:** C60-fullerene bound silica for the enrichment and the fractionation of multiphosphorylated peptides
Martin Fischnaller, Institute of Analytical Chemistry and Radiochemistry, Leopold-Franzens University, Innsbruck

18:10 **O10:** Conducting paths in lead zirconate titanate (PZT) after resistance degradation investigated by conductive AFM and other techniques
H. Ossmer, Institute of Chemical Technology and Analytics, Vienna University of Technology, Vienna

18:30 **O11:** Investigation of the formation of protein complexes by AFM
K. Bonazza, Institute of Chemical Technology and Analytics, Vienna University of Technology, Vienna

18:50 **Details zur Abendveranstaltung, Dankadresse an Sponsoren**

20:00 **Treffpunkt an der Naturwissenschaftlichen Fakultät (Haupteingang) zum gemeinsamen Aufbruch in die Altstadt**

20:30 **Abendveranstaltung im Sternbräu (Reservierung in der Kaiserstube auf ASAC), Griesgasse 23-25, Salzburg (siehe Lageplan im Anhang des Programms)**

8. ASAC JunganalytikerInnen Forum 01.06. – 02.06.2012

Programm

Samstag, 02.06.2012

ab 08:30 **Registrierung an der Naturwissenschaftlichen Fakultät (Erdgeschoß) im Foyer vor dem HS 403 (Grüner Hörsaal)**

Session 4: Nanostructures, sensors, & spectroscopy

Chair: Gunda Köllensperger & Victor Weiss

09:00 **O12:** Quantum cascade laser based optical sensors for chemical analyses in the liquid phase
Markus Brandstetter, Vienna University of Technology, Vienna

09:20 **O13:** Monitoring of proteinogenic biofilm growth on an evanescent wave photonic sensor
Eva Melnik, Health & Environment Department, AIT & Department of Analytical Chemistry, University of Vienna, Vienna

09:40 **O14:** Towards the detection of ATP levels above primary PTPRζ-osteoblastic cells and their knock-out mutants using amperometric ATP-microbiosensors
Charlotte Steinbach, Institute of Analytical and Bioanalytical Chemistry, University of Ulm, Ulm

10:00 **O15:** QCM Process Sensing of *E. coli* in a Bioreactor based on Imprinted Polymers
Renata Samardzic, Department of Analytical Chemistry, University of Vienna, Vienna

10:20 **O16:** Co-ordinative interactions – as the basis for designing Cu^{2+}-imprinted nanostructures
Sadia Zafar Bajwa, Department of Analytical Chemistry, University of Vienna, Vienna

10:40-11:00 **Kaffeepause im Foyer**

Session 5: Nanoparticles & spectroscopy

Chair: Gernot Friedbacher & Klaus Bonazza

11:00 **O17***:* Gas-Phase Electrophoretic Mobility Separation as a Tool for Sizing and Characterizing Nanoparticles
Angela Lehner, Institute of Chemical Technologies and Analytics, Vienna University of Technology, Vienna

11:20 **O18:** Advanced vibrational spectroscopic imaging of human tissue micro arrays containing cancer tissue in life science
Christine Pezzei, Institute of Analytical Chemistry and Radiochemistry, Leopold-Franzens University, Innsbruck

11:40 **O19:** Evaluation of hyperspectral imaging and classical vibrational spectroscopy for the quantification of furosemide polymorphs in ternary mixtures
Stefan A. Schönbichler, Institute of Analytical Chemistry and Radiochemistry Leopold-Franzens University, Innsbruck

Session 6 (Part 1): HPLC, HPLC-MS

Chair: Martina Marchetti-Deschmann & Jürgen Scheer

12:00 **O20:** HILIC: A systematic column characterization
Georg Schuster, Department of Analytical Chemistry, University of Vienna, Vienna

12:20 **O21:** Novel aminophosphonate multimodal selectors for liquid chromatography based on UGI-multi-component reaction
Andrea Gargano, Department of Analytical Chemistry, University of Vienna, Vienna

12:40 **O22:** Identification and quantitation of hindered amine light stabilizers (HALS) by HPLC/MS or direct MS/MS
Michael Reisinger, Institute for Analytical Chemistry, Johannes Kepler-University, Linz

13:00-14:00 Mittagspause mit Catering im Foyer

Session 6 (Part 2): HPLC, HPLC-MS, Proteomics

Chair: Martina Marchetti-Deschmann & Jürgen Scheer

14:00 **O23:** Analytical characterisation (HPLC-MS) of biomass pretreated by the "steam explosion"-process
Thomas Schmid, Institute for Analytical Chemistry, Johannes Kepler University, Linz

14:20 **O24:** Analysis of the proteome of monocytic and dendritic cells
Melanie Rothauer, Division of Chemistry and Bioanalytics, Department of Molecular Biology, University of Salzburg, Salzburg

Session 7: Metabolites & Metabolomics

Chair: Michael Lämmerhofer & Helmut Hinterwirth

14:40 **O25:** LC-HRMS/MS based approach for the screening of microbial iron-containing metabolites (siderophores)
Sylvia M. Lehner, Center for Analytical Chemistry, Department for Agrobiotechnology (IFA-Tulln), University of Natural Resources and Life Sciences, Vienna

15:00 **O26:** GC-MS Based Metabolomics to Study *Fusarium* Head Blight
Denise Schöfbeck, Center for Analytical Chemistry, Department IFA-Tulln, University of Natural Resources and Life Sciences, Vienna

15:20 **O27:** *In vivo* ^{13}C labelling for the study of metabolite profiles of different strains *Fusarium graminearum* by LC/MS
Bernhard Kluger, Center for Analytical Chemistry, Department for Agrobiotechnology IFA-Tulln, University of Natural Resources and Life Sciences, Vienna

15:40 **O28***:* Pentahydroxyscirpene – detection, isolation, structure elucidation and toxicity assessment of a new mycotoxin
Elisabeth Varga, Center for Analytical Chemistry and Christian Doppler Laboratory for Mycotoxin Metabolism, Department for Agrobiotechnology (IFA-Tulln), University of Natural Resources and Life Sciences, Vienna

16:00 **O29:** LC-MS based method development for metabolomic analysis in human cell cultures
Ines C. Forstenlehner, Division of Chemistry and Bioanalytics, Department of Molecular Biology, University of Salzburg, Salzburg

16:20-16:40 Getränkepause & Jury Session

16:40 Auszeichnung der PreisträgerInnen

16:50 Dankadresse an die Sponsoren, Ankündigung des 9. ASAC JunganalytikerInnen Forums und Verabschiedung

17:00 Ende der Veranstaltung

Abstracts

Key Lecture: Testing in analytical chemistry – what can go wrong and what can we do about it?

M. Bickel

European Commission, DG JRC, Institute for Reference Materials and Measurements,
Retieseweg 111, B-2440 Geel, Belgium
E-mail: michael.bickel@ec.europa.eu

Errors, mistakes and irregularities are omnipresent – the more sophisticated our activity, the higher their probability. Analytical laboratories usually carry out VERY sophisticated activities hence they are VERY prone to such deviations. In addition, their consequences can be serious: economical losses, environmental pollution, creation of or aggravation to human health problems or even loss of lives.

Therefore, we are extremely interested in developing mitigating measures that reduce likelihood of errors and mistakes. How can we do that?

On the organisational side we rely on clear policies, clear structure, clear planning and the commitment of our management, and on our capability to assess ourselves and to learn from our own and others' mistakes.

On the technical side we rely on our scientific competence and good methods, delivering good results. What does the term "good" mean here? The presentation will elaborate on this question (to some extent) and will work out the basic pillars of a quality laboratory building that produces valid analytical results.

O1: Phosphorothioate Oligonucleotide Characterization by Micro Liquid Chromatography - Mass Spectrometry

Robert Erb[1], Katharina Leithner[2], Andreas Bernkop-Schnürch[2], Herbert Oberacher[1]

[1] Institute of Legal Medicine, Innsbruck Medical University, Muellerstrasse 44, 6020 Innsbruck, Austria
E-mail: Robert.Erb@i-med.ac.at.

[2] Department of Pharmaceutical Technology, Institute of Pharmacy, Leopold-Franzens-University Innsbruck, Innrain 52, Innsbruck, Austria

Phosporothioate oligonucleotides represent an important class of therapeutic oligonucleotides developed for the treatment of various diseases, including cancer, infectious diseases, cardiovascular disorders and neurodegenerative disorders. These oligonucleotides allow the modulation of expression of targeted genes. To enhance bioavailability and stability against degradation by exonucleases and endonucleases, none-bridging oxygen atoms of the phosphate groups are replaced by sulphur.

The development and application of therapeutical oligonucleotides require analytical support. For this reason an assay for the quantitative analysis of a phosporothioate oligonucleotide in rat plasma was developed. The two-step assay employs solid-phase extraction (SPE) for sample preparation and ion-pair reversed-phase liquid chromatography on a monolithic capillary column hyphenated to high-resolution tandem mass spectrometry for detection and quantification of nucleic acids. To obtain low limits of detection, SPE parameters, chromatographic parameters (e.g. column temperature and mobile phase composition) as well as mass spectrometric parameters (e.g. spray voltage, gas flow, and scan mode) were optimized. The setup allowed processing of only 10 µl of plasma. The five-point calibration curve showed linearity over the range of concentrations from 100 to 1000 nM of the oligonucleotide. The limit of detection was 50 nM. The intra- and inter-day precision and accuracies were always better than 10.2%. Using this assay, a pharmacokinetic study of the phosporothioate oligonucleotide in rat treated with a single intravenous dose was performed. Small amounts of the oligonucleotide were detectable up to 3 h after dosing, which clearly demonstrates that the developed assay offers sufficient sensitivity to study the early phase elimination of the oligonucleotide in rats.

O2: Comparison of different MS platforms for determination of mass isotopomer distribution in cellular samples

Guerrasio R.[1], Haberhauer-Troyer C.[2], Steiger M.[3], Sauer, M.[3], Koellensperger G. [2], Hann S.[2]

[1] Austrian Centre of Industrial Biotechnology (ACIB) c/o University of Natural Resources and Life Sciences – BOKU Vienna, Department of Chemistry, Division of Analytical Chemistry, Muthgasse 18, A-1190 Vienna, Austria
[2] University of Natural Resources and Life Sciences – BOKU Vienna, Department of Chemistry, Division of Analytical Chemistry, Muthgasse 18, A-1190 Vienna, Austria.
[3] University of Natural Resources and Life Sciences – BOKU Vienna, Department of Biotechnology, Muthgasse 18, A-1190 Vienna, Austria.

Introduction
Mass Isotopomer Distribution Analysis (MIDA) is nowadays a MS application involved in the field of Fluxomics, one the most promising fields in system biology. Quantification of uncertainty in analytical measurement is the methodology promoted by ISO, which defines uncertainty as the "parameter, associated with the result of a measurement that characterizes the dispersion of the values that could reasonably be attributed to the measurand". The final goal of this concept is to identify and quantitate all sources of uncertainty affecting the experiment for further improvement of the quality of analytical results.

In the present work we have investigated the uncertainty contribution of different mass spectrometric techniques (HPLC-TOF-MS, HPLC-MS/MS and GC-MS) to mass isotopomer distribution analysis (MIDA).

Methods: Mass Isotopomer Distribution Analysis (MIDA) via MS-based platforms.
The developed protocol comprised the growth of a wild type *Pichia pastoris* strain on a mixture of ^{13}C-fully labeled glucose/^{nat}C-glucose (10:90), the rapid harvesting of the cells and the immediate quenching of the metabolism in ice cold methanol. The metabolome was then extracted in boiling ethanol and processed in order to meet the requirements of GC-MS or LC-MS analysis. MID data quality is evaluated regarding accuracy and repeatability precision calculated over 5 repetitive injections and reproducibility.
Moreover, an uncertainty budget highlighting the contribution of different uncertainty sources was calculated according to the ISO/BIPM *Guide to the Expression of Uncertainty in Measurement.* A further validation study approach was performed with the evaluation of MID Probability Density Function (PDF) through a Monte Carlo Method (MCM).

Conclusions
All the three MS platforms show satisfactory performances (evaluated in terms of precision and accuracy) in measuring analytes MIDs. The study will reveal that the major uncertainty sources will be the reproducibility and repeatability precision which are representative of the random fluctuation within the chromatographic separation and the peak integration procedure. The MCM highlighted a Gaussian distribution of the measurands and confirmed the results coming from Measurement Uncertainty.

Novel aspect
For the first time, measurement uncertainty according to ISO/BIPM is used to assess different MS based methods in the context of Fluxomics.

Acknowledgement:

This work has been supported by the Austrian Center for Industrial Biotechnology (ACIB) Federal Ministry of Economy, Family and Youth (BMWFJ), the Federal Ministry of Traffic, Innovation and Technology (bmvit), the Styrian Business Promotion Agency SFG, the Standortagentur Tirol and ZIT - Technology Agency of the City of Vienna through the COMET-Funding Program managed by the Austrian Research Promotion Agency FFG.
EQBOKU VIBT GmbH is acknowledged for providing LC-MS/MS and GC-MS/MS instrumentation.

O3: QUALITY CONTROL of HUMAN RHINOVIRUS SEROTYPE 2 PREPARATIONS by ORTHOGONAL ANALYSIS METHODS

Victor U. Weiss[1, 2], Marlene Havlik[1], Irene Gösler[2], Xavier Subirats[2], Mohit Kumar[2], Ernst Kenndler[2], Dieter Blaas[2] and Günter Allmaier[1]

[1] Institute for Chemical Technologies and Analytics, Vienna University of Technology, Getreidemarkt 9/164 IAC, 1060 Vienna, Austria
E-mail: victor.weiss@tuwien.ac.at
[2] Max F. Perutz Laboratories, Department of Medical Biochemistry, Medical University of Vienna, Dr. Bohr Gasse 9/3, 1030 Vienna, Austria

Human Rhinoviruses (HRVs), members of the Picornavirus family causing common cold infections, are non-enveloped icosahedral particles of approx. 30 nm diameter and are formed of 60 copies each of four viral proteins and a single stranded RNA genome [1]. HRV caused infections are usually relatively mild, however, other *Picornaviridae,* like hepatitis-A- or poliovirus, account for more severe infections. These reasons predestine HRVs as model to study early viral infection steps ranging from receptor mediated endocytosis to the RNA transfer process into the cytosol of an infected cell.

Although already much is known about HRVs, especially for serotype 2 (HRV2) (e.g. lately the X-Ray structure of the endpoint of viral cell infection was published [2]), still many questions remain. Beside others these include for instance the exact mechanisms of how HRVs are able to transfer their RNA through the endosomal membrane into the cytosol of an infected cell. To target these questions, well defined virus material is required. Within our presentation we demonstrate the application of several orthogonal methods - $TCID_{50}$, capillary electrophoresis (CE, both conventional as well as in the chip format), transmission electron microscopy (TEM) and gas phase electrophoretic mobility molecular analysis (GEMMA) - in the quality control of HRV2 preparations. We found a contamination of HRV2 material to be related to lipids, possibly exosomes, co-purified with virions [3]. Especially for investigation of membrane associated early viral infection steps, such lipid contaminations might result in interferences. Thus, the removal of such contaminations (also for preparation of highly pure samples as needed for exact molecular weight determination of intact virus assemblies [4] via nano electrospray ionization IM QqRTOF mass spectrometry) is of great importance.

REFERENCES

[1] Fuchs, R.; Blaas, D., *"Uncoating of human rhinoviruses"*, Reviews in Medical Virology **20** (5), 281-297 (2010)

[2] Garriga, D.; Pickl-Herk, A.; Luque, D.; et al, *"Insights into minor group rhinovirus uncoating: the X-ray structure of the HRV2 empty capsid"*, PLoS Pathogens **8** (1), e1002473 (2012)

[3] Weiss, V. U.; Subirats, X.; Pickl-Herk, A.; et al, *"Characterization of Rhinovirus Subviral A-Particles via Capillary Electrophoresis, Electron Microscopy and Gas Phase Electrophoretic Mobility Molecular Analysis. Part I"*, Electrophoresis, accepted (2012)

[4] Uetrecht, C.; Versluis, C.; Watts, N.R.; et al, *"High-resolution mass spectrometry of viral assemblies: Molecular composition and stability of dimorphic hepatitis B virus capsids"*, Proceedings of the National Academy of Sciences of the United States of America **105** (27), 9216-9220 (2008)

Acknowledgements:
Austrian Science Foundation (FWF) - grants P18693-B09, P19365, P20915-B13, APW01221FW and TRP29-N20; Government of Catalonia - grant 2008BPA00029; Medical University of Vienna - DK Structure and Interaction of Biological Macromolecules

O4: Application of CIEF for the Characterization of Proteins/Allergens

Theresa Kristl[1], Hanno Stutz[1]

[1] Division of Chemistry and Bioanalytics, Department of Molecular Biology, University of Salzburg, Hellbrunner Str. 34, A-5020 Salzburg, Austria
E-mail: kristltheresa@gmx.at

Biopharmaceutical companies as well as academic research progressively require a comprehensive characterization of applied protein/allergen products. Profiling and composition elucidation of applied source materials represents a prerequisite for interpretation of research results [1]. Analytical methods feasible for the characterization of biological and biotechnological proteins/ allergens, are exemplified in the ICH guideline Q6B which explicitly mentions capillary electrophoresis (CE) [2]. Among the different CE modes, capillary isoelectric focusing (CIEF) is considered to provide an outstanding selectivity which allows for a resolution of proteins or peptides differing in their isoelectric points (p*I*s) by only 0.02 units or even less.

Beside airborne allergens, food allergens constitute a key trigger for allergic disorders particularly in infancy. Ovalbumin, the major protein of chicken-egg white, represents a prominent causative source for food allergies. Due to various post-translational modifications, *e.g., N*-glycosylation, acetylation and phosphorylation, ovalbumin possesses a pronounced heterogeneity [3]. The complex composition of commercial products promotes the application of high-selectivity separations, such as CIEF.

Development, optimization and validation of CIEF methods were performed on a recently launched CE system. For the mobilization of focused protein zones towards the detector different strategies were employed and optimized, including the application of pressure or addition of appropriate reagents to one electrolyte vessel. For either mobilization strategy, method settings and separation parameters were comprehensively tested to optimize the resolution for ovalbumin products. Naturally, the pH gradient gradually shifts over time, which is caused by the so-called plateau phenomenon as well as by cathodic and anodic drifts. Spacer compounds focused on either end of the capillary can reduce this sort of instabilities. Delicate combinations of wide and narrow pH range carrier ampholytes were required to assure the resolution of target allergen variants. The p*I*s of resolved ovalbumin fractions were calculated by synthetic peptides with their p*I* tailored to flank the allergen cluster closely. Different commercial products, including a crude lysate, were analyzed by CIEF, and compared with results derived by CZE and ESI-TOF MS.

REFERENCES

[1] Kronsteiner, B., H.J. Malissa, and H. Stutz, *Profiling recombinant major birch pollen allergen Bet v 1a* and carbamylated variants with CZE and CIEF. Electrophoresis, 2007. **28**(13): p. 2241-51.

[2] *ICH Guideline Q6B - Specifications; Test Procedures and Acceptance Criteria for Biotechnological/Biological Products.* 1999: p. 1-16.

[3] Harvey, D., et al., *Composition of N-linked carbohydrates from ovalbumin and co-purified glycoproteins.* Journal of the American Society for Mass Spectrometry, 2000. **11**(6): p. 564-571.

Acknowledgements:

This work was performed within a Research Sponsoring Agreement (RSA) between Agilent Technologies and the University of Salzburg. Within the RSA an *Agilent 7100 Capillary Electrophoresis System* was provided as a loaner. Dr. Martin GREINER, Dr. Gerard ROZING, and Dr. Hans-Josef BRUNNERT (all from *Agilent Technologies*, Waldbronn, Germany) are gratefully acknowledged for their continuous support and technical assistance.

O5: Characterization of Nitrated Allergens by Various Capillary Electrophoresis Modes

Sergey Gusenkov[1], Chloé Ackaert[2], Gertie J. Oostingh[2], Hanno Stutz[1]

[1] Division of Chemistry and Bioanalytics, Department of Molecular Biology, University of Salzburg, Hellbrunner Str. 34, 5020 Salzburg, Austria
E-mail: sergey.gusenkov@sbg.ac.at
[2] Division of Allergy and Immunology, Department of Molecular Biology, University of Salzburg Hellbrunner Str. 34, 5020 Salzburg, Austria

The increase in allergic disorders over the past decades has developed in a pronounced issue of concern for public health systems of industrialized societies. Currently, more than 17 million people are affected by allergies in Europe [1].The major birch pollen allergen Bet v 1a represents one of the most prominent airborne allergens. Chemical modifications, *i.e.,* nitration, of allergens can be induced either by environmental pollutants [2] or during endogenous inflammatory processes after their uptake [3]. Allergen nitration has been attributed to promote the allergenicity since it is suspected to trigger immune reactions [2]. In case of inflammations, peroxynitrite is produced and generates secondary radicals, *e.g.* $^{\bullet}NO_2$, by reaction with CO_2 or homolysis of peroxynitrous acid [4,5]. In correspondence with certain conditions nitration predominantly occurs at tyrosine residues. Therefore, in-lab nitrated allergens in defined quality are required as model compounds [6]. Since modification/nitration generates complex mixtures of closely related allergen variants, analytical tools of outstanding selectivity are compulsory and should additionally cover multiple aspects of physico-chemical characterization. The combination of various CE modes is predestined to tackle this task. CZE in dynamically modified capillaries and CIEF employing a mixture of wide and narrow pH range carrier ampholytes, both with UV detection, provide orthogonal results in profiling nitration products. These CE modes equally allow for an evaluation of the nitration grades, since nitration is accompanied by stepwise reduction in the isoelectric point. Peak assignment to nitrated species is accessible by CZE-ESI-μTOF MS. Combinations of various CE techniques and detection modes provide orthogonal information in terms of physicochemical properties (*e.g.* p*I*, M_r), purity, nitration profiles and abundance of nitrated species. In combination, this assures a comprehensive product characterization.

REFERENCES

[1] http://www.eaaci.net/eaacimedia

[2] Franze, T., Weller, MG, Niessner, R., Pöschl, U.,"*Protein nitration by polluted air*", Environmental Science and Technology **39**, 1673-1678 (2005)

[3] Van der Vliet, A., Eiserich, J.P., Shigenaga, M.K., Cross, C.E., "*Reactive nitrogen species and tyrosine nitration in the respiratory tract: epiphenomena or a pathobiologic mechanism of disease?*", American Journal of Respiratory and Critical Care Medicine **160**, 1-9 (1999)

[4] Lancaster,R. Jr.,*"Nitroxidative, nitrosative, and nitrative stress: kinetic predictions of reactive nitrogen species chemistry under biological conditions",*Chemical Research in Toxicology**19**(9), 1160-1174 (2006)

[5] Alvarez, B.,Radi, R., "Peroxynitrite reactivity with amino acids and proteins" *Amino Acids*, **25** (3-4), 295-311 (2003)

[6] Bruice, TC., Gregory, MJ., Walters, SL., *"Reaction of tetranitromethane. I. Kinetics and mechanism of nitration of phenols by tetranitromethane",* Journal of American Chemical Society **90,** 1612-1619 (1968)

Acknowledgements:

This work was supported by grant No. P22236 of the Austrian Science Fund (FWF).

O6: CE and CE-ESI-MS Studies to Elucidate the Hydrolysis Behavior of AnticancerBis(acetoxime)dihalidoplatinum(II) Complexes

G. Grabmann[1], S. M. Meier[1,2], Y. Y. Scaffidi-Domianello[1], M. Galanski[1], B. K. Keppler[1,2], C. G. Hartinger[1-3]

[1] University of Vienna, Institute of Inorganic Chemistry, Währinger Str. 42, 1090 Vienna, Austria
E-mail: gerlinde.grabmann@univie.ac.at
[2] Translational Cancer Therapy Research, Währinger Str. 42, 1090 Vienna, Austria
[3] The University of Auckland, School of Chemical Sciences,Private Bag 92019, Auckland 1142, New Zealand

Since the discovery of cisplatin as a potent anticancer drug, much effort has been devoted to the development of anticancer agents with improved anticancer activity, toxicity and resistance profiles. Carboplatin and oxaliplatin followed the lead structure of cisplatin and were approved by the FDA a few decades later. However, side effects and resistance problems have not been overcome so far. More recently, research has been focused on metallodrugs with different modes of action and especially rule-breaking compounds such as *trans*-configured complexes are highly sought after [1].
A novel group of *cis*- and *trans*-[bis(acetoxime)dihalidoplatinum(II)] (halido = Cl, Br, I) complexes has been recently developed and studied on their cellular accumulation, *in vitro* anticancer activity and DNA interaction [2]. Herein we compare the time-dependent hydrolysis of these compounds under simulated physiological conditions using capillary electrophoresis (CE). Hydrolysis products were identified using CE hyphenated to electrospray ionisation-mass spectrometry (ESI-MS). Significantly different behavior of the isomers was observed with a notable influence of the halido leaving group on the hydrolysis kinetics and the formation of hydrolysis products.

REFERENCES

[1] Jakupec, M., et al.,*Tumour-inhibiting platinum complexes—state of the art and future perspectives, Reviews of Physiology, Biochemistry and Pharmacology*. 2003, Springer Berlin Heidelberg. p. 1-53.

[2] Bartel, C., et al., *Cellular accumulation and DNA interaction studies of cytotoxic trans & cis - platinum anticancer compounds.* Journal of Biological Inorganic Chemistry, 2012. 17(3): p. 465-474.

Acknowledgements:

We would like to thank the University of Vienna for a PhD scholarship for G.G.within the doctoral program BioProMoTION (Bioactivity Profiling and Metabolism)and the Austrian Science Fund (FWF, project number I496-B11) for financial support.

O7: Quantitative determination of cisplatin-protein interaction in cell models by LC-ICP-MS

G. Hermann[1], P. Heffeter[1], W. Berger[2], S. Hann[1] and G. Koellensperger[1]

[1] Division of Analytical Chemistry, Department of Chemistry, University of Natural Resources and Life Sciences, Muthgasse 18, A-1190 Vienna, Austria.
E-mail: gunda.koellensperger@boku.ac.at
[2] Institute of Cancer Research, Department of Medicine I, Medical University Vienna, Borschkegasse 8a, 1090 Vienna, Austria

Since the introduction of cisplatin in chemotherapy, we keep learning about the cytostatic activity of the drug and its involvement into multiple biochemical pathways. The knowledge on the intracellular chemistry of the drug is based on assumptions, deduced from in vitro solution chemistry. It is safe to assume that cisplatin being an electrophile will form adducts with thiol- containing biomolecule once inside the cell. The question whether the adduct formation can be related to mechanisms of drug resistance, was not addressed by measurement so far. In this work, interaction between cytosolic proteins and low molar mass thiols was studied by elemental speciation approaches in cell models. (Pre)clinical relevant drug concentration levels were studied implementing isotope dilution strategies by LC-ICP-MS. The role of Glutathione in sensitive versus resistance cancer cell models was studied. ICP-MS addressed the quantification of drug uptake, intracellular distribution and quantification of protein bound drug versus low molar mass fraction. Determination of the intact and free drug was performed by LC-ICP-MS. Chromatographic separation of cisplatin species was based on pentafluorophenylpropyl-siloxane bonded- and on porous graphitic carbon stationary phases. Glutathione in reduced and oxidized form were studied by HILIC-MS-MS using isotopically enriched standards.

O8: HIGHLY SELECTIVE ISOLATION of PHOSPHOPROTEINS USING TRIVALENT LANTHANIDE-ION PRECIPITATION

Yüksel Güzel[1], Munazza Raza[1], Matthias Rainer[1] and Günther K. Bonn[1]

[1]Institute of Analytical Chemistry and Radiochemistry, Leopold-Franzens University, Innrain 52a, 6020 Innsbruck, Austria.
E-mail: Yueksel.Guezel@uibk.ac.at

Reversible phosphorylation of proteins plays a significant role in cellular processes including regulation of cellular functions, such as growth, metabolism and differentiation [1]. One of the major functions of phosphorylation is to act as a control to turn on or off a protein activity or cellular pathway in an acute and reversible manner. Since the discovery of phosphorylation as a key regulatory mechanism of cell life, the analysis of the entire phosphoproteome has become an attractive study [2].

This study describes a highly efficient method for the selective precipitation of phosphoproteins by trivalent lanthanide metal ions [3]. These metal cations belong to the group of lanthanides and are known to be hard “acceptors” with an overwhelming preference for oxygen-containing anions such as phosphates to which they form very tight ionic bonds. The method could be successfully applied to specifically precipitate phosphoproteins from complex samples including milk and egg-white by forming solid metal-protein complexes [4]. Due to the low solubility product of the investigated lanthanide salts, the produced metal-protein complexes showed high stability [5]. The protein pellets were extensively washed to remove non-phosphorylated proteins and contaminants. For the analysis of proteins the pellets were first dissolved in 30% formic acid and subjected to MALDI-TOF MS. For peptide mass-fingerprint analysis the precipitated phosphoproteins were enzymatically digested using microwave-assisted digestion. The method was found to be highly specific for the isolation and purification of phosphoproteins. Protein quantification was performed by colorimetric detection of total precipitated phosphoproteins and revealed more than 95% protein recovery for each lanthanide salt.

REFERENCES

[1] Manning, G., Whyte, DB., Martinez, R., Hunter, T., Sudarsanam, S., *“The protein kinase complement of the human genome”*, Science **298** (5600):1912 (2002)

[2] Delom, F., Chevet, E., *“Phosphoprotein analysis: from proteins to proteomes. Proteome”*, Science **4** (1):15 (2006)

[3] Güzel, Y., Rainer, M., Raza, MM., Bonn, GK., *“Highly efficient precipitation of phospho-proteins using trivalent europium, terbium, and erbium ions”*, Anal Bioanal Chem (2012, in press)

[4] Mine, Y., *“Recent advances in the understanding of egg white protein functionality”*, Trends in Food Science & Technology, **6** (7): p. 225-232 (1995)

[5] Liu, X., Byrne, RH., *“Rare earth and yttrium phosphate solubilities in aqueous solution”. Geochim Cosmochim Acta* **61** (8):1625–1633 (1997)

Acknowledgements:

This study was funded by the FWF-SFB Project 021 (Vienna, Austria).

O9: C60-fullerene Bound Silica for the Enrichment and the Fractionation of Multiphosphorylated Peptides

Martin Fischnaller, Rania Bakry and Günther K. Bonn

Institute of Analytical Chemistry and Radiochemistry, Leopold-Franzens University,
Innrain 80-82, 6020 Innsbruck, Austria
E-mail: Martin.Fischnaller@uibk.ac.at

Protein phosphorylation is one of the most important post translational modifications involved in a variety of biological processes such as proliferation, differentiation and apoptosis. Mass spectrometry of phosphopeptides obtained from tryptic protein digests is the method-of-choice for characterization of majority of the phosphorylated proteins. However, it is difficult to analyze phosphopeptides by MS, especially in the presence of the non-modified peptides. Due to lower ionization efficiency of phospopeptides, as well as the stoichiometry of phosphorylation is often present at low relative abundance, efficient enrichment of the phosphorylated peptides prior to MS analysis is of high demand. In addition, successful identification of multi-phosphorylated peptides still remains a challenging.

This work demonstrates a new strategy for the enrichment and subsequent selective elution of multi-, mono- and non-phosphorylated peptides, based on difference in pI of the phosphopeptides by using pH gradient elution with acetonitrile prior to matrix-assisted laser desorption/ionization time-of-flight mass spectrometer analysis. The developed protocol is successfully applied for α-casein tryptic digest, bovine serum albumin digest spiked with ten synthetic phosphopeptides and a tryptic milk digest.

O10: Conducting paths in lead zirconate titanate (PZT) after resistance degradation investigated by conductive AFM and other techniques

H. Ossmer, L. Andrejs, G. Friedbacher and J. Fleig

Institut für Chemische Technologien und Analytik, Technische Universität Wien, Getreidemarkt 9/164, 1060 Wien
E-mail: hinnerk.ossmer@tuwien.ac.at

Lead zirconate titanate (PZT) is one of the most important piezoelectric materials and used in applications such as actuators, sensors or ultra sound transducers. It is known to suffer from different kinds of degradation including fatigue, aging and loss of insulation resistance [1]. All these degradation phenomena include complex kinetic processes and are not completely understood yet. Particularly resistance degradation seems to be an effect that could be caused by different, possibly independent processes. In this contribution, we present results on the resistance degradation of donor doped PZT, taking place at temperatures between 350 and 520°C. Samples were cut from actuator stacks with Ag/Pd inner electrodes. Several methods were employed to analyze surface precipitates, as well as location and nature of current paths appearing upon fields of about 1 kV/cm after tens of minutes up to several days of degradation. Conductive structures were detected on the surface by means of conductive AFM (C-AFM). Mechanical removal of near-surface layers revealed the depth distribution of the conducting paths in dependence of temperature, time and electric field. C-AFM measurements with high resolution and slow scan rates were employed to further specify and monitor the local distribution of the paths and their correlation to the surface precipitates. The role of grain boundaries in the degradation process will also be discussed. SEM and EDX revealed the surface precipitates to consist of Ag and/or Pb rich structures. Additionally, in degraded layers the Ag content of anodic electrodes was found to decrease and an enhanced porosity of anodes was observed. Coloration effects accompanying the degradation were investigated in dark field optical microscopy, but do not seem to be related to the massive resistance drop of the material.

REFERENCES

[1] E. Völkl, P. Hillebrand, J. Fleig, *"Resistance variation in donor-doped PZT stacks with Cu inner electrodes under high field stress*", Journal of Electroceramics **27** (2), 66-77 (2011)

Acknowledgements:

We gratefully acknowledge the *Christian Doppler Society* for funding and thank Mrs. E. Eitenberger for acquisition of SEM data.

O11: Investigation of the formation of protein complexes by AFM

K. Bonazza[1], H. Rottensteiner[2], B. Seyfried[2], G. Allmaier[1], P.L. Turecek[2], and G. Friedbacher[1]

[1] Institute of Chemical Technology and Analytics, Vienna University of Technology, A-1060 Wien, Getreidemarkt 9/164-IAC
E-mail: e0325540@student.tuwien.ac.at
[2] Baxter Innovations, A-1221 Wien, Industriestraße 67

Von Willebrand Factor (vWF) is the largest glycoprotein in human blood playing a twofold role in haemostasis. On the one hand it acts as a linker to cause adhesion of blood platelets to sub-endothelial cells, on the other hand it stabilizes the FVIII in the circulation [1] by forming a tight non-covalent complex. VWF circulates mainly as a large multimer consisting of an average number of 20 dimer units. Although numerous investigations on the formation of the VWF-FVIII complex can be found in literature, images proving the specific binding do not exist yet. Images of pure vWF have first been obtained with AFM in 1992 [2]. VWF immobilized on mica shows repeating globular structures with interconnecting rod-like regions [3]. Recently, AFM has been used to image gold labelled vWF enabling its detection on rough surfaces like immobilized collagen [4], and also force spectroscopy has been performed revealing new insights in the cleavage of stretched vWF multimers induced by the protease ADAMTS13 [5].

In this work the formation of the VWF-FVIII complex is imaged by AFM using a novel preparation method to follow up protein reactions on the single molecule level. Our approach allows obtaining an image of exactly the same molecule before and after the complex formation. This system is particularly difficult to study by imaging, since the globular FVIII molecules differ from the globular domains of vWF only by a factor of 1-1.5 in diameter necessitating to maintain the position of the vWF-chain during the complex formation as much as possible in order to compare every individual globular domain before complex formation and thereafter. For this purpose a new approach for the investigation of the adhesion of vWF on mica in the presence of a buffer liquid has been developed and measures were taken to optimize the surface interaction. We show that the FVIII binding capacity of vWF is not limited to one mol FVIII per mol vWF.

REFERENCES

[1] Sadler, J.E., *"Von Willebrand Factor"* The Journal of Biological Chemistry **266** (34), 22777-22780 (1991)

[2] Raghavachari, M., *"Surface dependent structures of von Willebrand factor observed by AFM under aqueous conditions"* Colloids and Surfaces B: Biointerfaces **19** (4) 315-324 (2000)

[3] Marchant, R.E., *"Interactions of von Willebrand factor on mica studied by atomic force microscopy"* Journal of Colloid and Interface Science **148** (1), 261-272 (1992)

[4] Novák, L *"Shear-dependent morphology of von Willebrand factor bound to immobilized collagen"* Blood **99**, 2070-2076 (2002)

[5] Tao, W., *"Force-induced cleavage of single vWF A1A2A3 tridomains by ADAMTS-13"* Blood, **115** (2), 370-378 (2010)

Acknowledgements:

We thank Gerald Schrenk, Stefan Haider, and Gerald Brachtl for excellent technical support.

Programm

Samstag 02.Juni 2012

O12: Quantum cascade laser based optical sensors for chemical analyses in the liquid phase

M. Brandstetter[1], A. Genner[1], G. Ramer[1], J. Kasberger[2], B. Lendl[1]

[1] Vienna University of Technology, Getreidemarkt 9/164AC, 1060 Wien,
E-mail: blendl@tuwien.ac.at
[2] Research Center for Non Destructive Testing GmbH, Altenberger Straße 69, A-4040 Linz

The implementation of mid-IR Quantum Cascade Lasers (QCL) in liquid phase absorption spectroscopy opens a broad field of potential applications, e.g. in clinical analysis and process analytical chemistry [1]. There, the key features of QCLs, such as high spectral power density and compact design make them suitable for portable sensor applications.

In liquid phase spectroscopy with QCLs tunability and high emission power are crucial, especially when measuring in highly absorbing matrices, e.g. in water. Both requirements were met by the employed broadly tunable External Cavity QCL (EC-QCL). An essential step towards high reproducibility in the measurements using this new mid-IR laser source was a thorough investigation of its time-resolved spectral characteristics. This was achieved using step-scan FTIR measurements in order to characterize pulse-to-pulse power fluctuations and spectral non-linearities.

An alternative approach to EC-QCLs can be the use of arrays of single-mode QCLs. In this context novel surface-emitting ring-cavity QCLs [2] are promising tools. Due to their ring-cavity design they offer enhanced emission characteristics compared to standard Distributed Feedback (DFB) QCLs. Moreover they enable compact sensor designs as they emit at very low divergences, which could make the use of lenses obsolete.

Furthermore, emerging technologies such as single-mode slab-waveguides (which offer a higher interaction pathlength with the evanescent field) for surface sensitive sensor concepts will be discussed. The combination of QCLs with these single-mode waveguides can facilitate compact sensor setups with the advantage of an enhanced sensitivity compared to conventional ATR measurements.

REFERENCES

[1] Brandstetter, M., *"Tunable external cavity quantum cascade laser for the simultaneous determination of glucose and lactate in aqueous phase*", Analyst **135**, 3260-3265 (2010)

[2] Mujagic, E., *"Ring-cavity surface emitting lasers as a building block for tunable and coherent quantum cascade laser arrays "*, Semicond. Sci. Technol., **26**, 1-6 (2011)

Acknowledgements:

Financial support was provided by the Austrian research funding association (FFG) under the scope of the COMET programme within the research network "Process Analytical Chemistry (PAC)"

O13: Monitoring of proteinogenic biofilm growth on an evanescent wave photonic sensor

E. Melnik[1,2], P. Muellner[1], R. Bruck[1], R. Hainberger[1], M. Laemmerhofer[2]

[1] AIT, Health & Environment Department, 1220 Vienna, Austria
[2] University of Vienna, Department of Analytical Chemistry, 1090 Vienna, Austria

Evanescent wave photonic sensors are optical waveguide sensors which exploit the exponentially decaying evanescent field of light that penetrates into the surrounding media (Fig. 1a)). The sensing principle relies on induced changes of the phase velocity of the guided laser light in the waveguide during the binding of analyte molecules to the functionalized surface. This sensing principle enables sensitive label-free real-time monitoring of biomolecular interactions.
In the past, different integrated optical transducers, such as ring resonators [1], gratings [2], and Mach-Zehnder interferometers [3], have been developed. In our work, we use amorphous hydrogenated silicon based Mach-Zehnder interferometric (a-Si:H-MZI) sensors (see Fig. 1b)), which serves as model system for evanescent wave sensors. The surface sensitivity of these sensors is determined by the refractive index of the materials, the waveguide cross section and the measurement wavelength [4,5].
In our resent work, we monitor proteinogenic biofilm growth by multi layer biotinylated bovine serum albumin/streptavidin biofilm deposition, which allows studying the correlation of the evanescent field profile, the biofilm packing density and the MZI signal. This research is important for the biosensor development in order to maximizing the chemical sensor sensitivity.

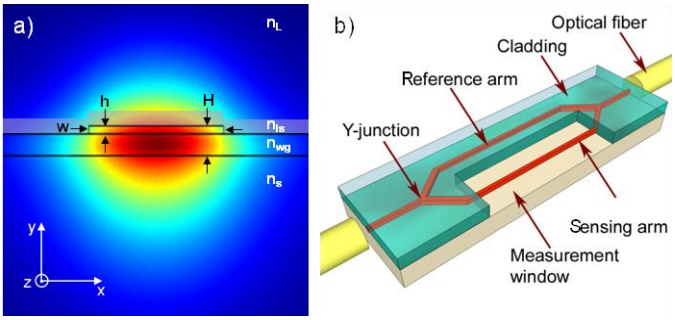

Fig. 1. a) Cross section, optical power distribution and parameters of rib waveguide structure. Rib width *w*=1.8µm, height of the rib waveguide *h*=5 nm, height of the waveguide layer *H*=80nm, refractive index of the substrate n_S=1.46, waveguide n_{wg}=3.48, the layer stack n_{ls}=1.46, measurement liquid n_L=1.33; b) MZI structure with end face coupling via optical fibers.

In the best knowledge of the authors, so far only one study, performed by Luchansky et al. [6], has addressed this issue. In contrast to their work we address highly relevant open issues such as the biofilm height and refractive index under the used measurement conditions by numerically solving the eigenmode equation of the optical four layer slab waveguide system. The measured start values for the calculation are the thickness of the waveguide layer and the streptavidin start layer packing density, which are measured with scanning electron microscopy and fluorescence scans, respectively. Furthermore, control measurements with atomic force microscopy and X-ray photoelectron spectroscopy were performed. Over this study, we give an empirical approach to determine the refractive index and layer height of a proteinogenic biofilm directly on evanescent wave sensors.

REFERENCES

[1] De Vos, K., et al., Opt. Express **15** 7610–7615 (2007).
[2] Waldhäusl, R., et al., Appl. Opt. **36** 9383–9390 (1997).
[3] Heideman, R. G., et al., Sens. Actuators. B Chem. **10** 209–217 (1993).
[4] Tiefenthaler, K., et al., J. Opt. Soc. Am. B **6** 209–220 (1989).
[5] Parriaux, O., et al., IEEE J. Lightwave Technol. **16** 573–582 (1998).
[6] Luchansky, M. S., et al., Biosens. Bioelectron. **26** 1283-1291 (2010).

Acknowledgements:

This research was supported through the grant PLATON Si-N (project no. 819655) funded by the Austrian NANO Initiative.

O14: Towards the detection of ATP levels above primary PTPRζ-osteoblastic cells and their knock-out mutants using amperometric ATP-microbiosensors

Charlotte Steinbach[1], Elena Hecht[1], Astrid Liedert[2], Anita Ignatius[2], Boris Mizaikoff[1] and Christine Kranz[1]

[1] Institute of Analytical and Bioanalytical Chemistry, University of Ulm, Albert-Einstein-Allee 11 89081 Ulm, Germany
E-mail: charlotte.steinbach@uni-ulm.de
[2] Institute of Orthopaedic Research and Biomechanics, University of Ulm, Helmholtzstraße 14 89081 Ulm, Germany

Adenosine-5`-triphosphate (ATP) holds a significant role as omnipresent energy source and as autocrine and paracrine signaling molecule in many cells such as lung cells and bone cells [1]. ATP is considered to be involved in the mechanical stress response of bone cells such as bone-resorbing osteoblast cells or receptor-proteine-tyrosine-phosphatase-zeta (PTPRζ) - osteoblastic cells [2], which are involved in bone formation, bone regeneration and the control of bone volume. ATP release stimulates the proliferation of these P2 - receptor cell types [3,4]. The "deficient" knock-out mutant behaves different in proliferation and differentiation and thus the ATP release above these cells is expected to be altered. A localized detection of ATP at the cellular level is therefore of significant importance. Using amperometric ATP microbiosensors with diameters ranging from 10 - 50 µm enables localized ATP measurements above wild type and knock-out cells.

The determination of ATP is based on a competitive assay with glucose converting oxidoreductases (e.g. GOD or PQQ-GDH) and hexokinase (HEX) immobilized at the surface of the microelectrode (5,6). Experiments were conducted in a three-electrode setup in combination with a scanning electrochemical microscope for positioning the biosensor close to the cell surface. A dual microelectrode assembly served as working electrodes (WEs), using one electrode for positioning and the second as transducer for the microbiosensor. First results describing cultivation and experimental setup on localized ATP measurements above osteoblasts and (PTPRζ) - osteoblastic cells will be presented and discussed.

REFERENCES

[1] N.R. Jorgensen, S.T. Geist, R. Civitelli, T.H. Steinberg, *J Cell Biol 139,* (**1997**), 497–506

[2] K.A. Buckley, S.L. Golding, J.M. Rice, J.P. Dillon, J.A. Gallagher, *The FASEB Journal (17)*, (**2003**), 1406

[3] T. Schinke, M. Gebauer, A.F. Schilling, S. Lamprianou, M. Priemel, C. Mueldner, C. Neunaber, T. Streichert, A. Ignatius, S. Harroch, M. Amling, *Bone 42*, (**2008**) 524**–**534

[4] J.A. Gallagher, *J Musculoskel Neuron Interact, 4(2*), (**2004**), 125-127

[5] A. Kueng, C. Kranz, B. Mizaikoff, *Biosensors and Bioelectronics, 21*, (**2005**), 346-353J.-F. Masson, C. Kranz, B. Mizaikoff, E. B. Gauda, *Anal. Chem. 80,* (**2008**), 3991–3998

[6] C. Weber, E. Gauda, B. Mizaikoff, C. Kranz, *Anal Bioanal Chem, 395* (**2009**) 1729**–**1735

O15: QCM Process Sensing of E. coli in a Bioreactor based on Imprinted Polymers

Renata Samardzic[1], Nathjanan Jongkon[2] and Peter Lieberzeit[3]

[1] Universität Wien, Währinger Straße 38, 1090 Wien, Austria
E-mail: renata.samardzic@univie.ac.at
[2] Department of Social and Applied Science, College of Industrial Technology, The King Mongkut's University of Technology, 10800 Bangkok, Thailand
[3] Universität Wien, Währinger Straße 38, 1090 Wien, Austria
e-mail: peter.lieberzeit@univie.ac.at

Designing robust sensor systems aiming at measurements in real-life matrices is a substantial challenge. This requires special attention to factors such as ruggedness, stability, sensitivity and selectivity of the sensor. Therefore artificial receptor materials are of substantial interest. They can be based e.g. on bulk and surface imprinted polymers [1]. For designing molecularly imprinted polymers (MIP) based on polyurethane as synthetic receptors for QCM sensing of biological agents, we focused on *E. coli* as a model species including different strains (b and w). *E. coli* is a gram-negative bacterium, anaerobic and ranges in size from 1 µm till 3 µm. MIP optimized to selectively recognize *E. coli* showed ten times higher responses on QCM than the non-imprinted polymers. The selectivity of *E. coli* in the concentration range of 0.1 mg/ml-5 mg/ml ($8*10^8$ cells/ml – $4*10^{10}$ cells/ml) in aqueous solution is determined by combination of functional and geometrical properties, as bacteria of strain w are slightly larger than those of strain b. For the w-strain MIP, the response towards its own analyte (concentration range 0.1 mg/ml - 5 mg/ml) covers a range from 100 Hz to 2200 Hz. For the b- strain MIP it is 200 Hz and 5000Hz. The selectivity between the strains reaches a factor of 2. As a consequence of this, layers were optimized for long-term use to address real-life sensing. Optimization mainly concerned the amount of the cross-linkers, which was changed from 5.2 mg to 4.3 mg. The results for the b-strain MIP are as follows: for a concentration of 1 mg/ml the new sensor yielded 1200 Hz response, after 6 months 1000 Hz and after one year 800 Hz. For the w- strain *E. coli* MIP and a concentration of 1mg/ml, at the beginning it was 600 Hz, after 6 months 500 Hz and after one year 500 Hz. We also investigated the reproducibility of both individual sensors and between different batches and obtained appreciable results. Finally, a bioreactor setup for measuring breeding of *E. coli* at real-life conditions (multiplying every 20 min. at 37°C in culture medium) was developed for measurements in flow mode. We undertook in-situ experiments with starting concentrations from 0.08 mg/ml -1 g/ml of w-and b- strain, respectively, as well as assessing selectivity, mixtures of different strains and measurements over several days. E.g. b- strain *E. coli* with concentration of 80 mg/ml give response of 16850 Hz and w- strain *E. coli* a response of 20590 Hz after 45 minutes of breeding.

REFERENCES

[1] A. Findeisen, J. Wackerlig, R. Samardzic, J. Pitkänen, O. Anttalainen, F. L. Dickert, P. A. Lieberzeit: *"Artifical receptor layers for detecting chemical and biological agent mimics"*, 1, (2011)

Acknowledgements:

The work presented here has been funded by the European Commission via the Sixth Framework Program, project EU-FP6 NMP3-CT-2006-026549 "NANOSECURE", which we gratefully acknowledge.

O16: Co-ordinative Interactions – as the Basis for Designing Cu^{2+}-Imprinted Nanostructures

Sadia Zafar Bajwa[1] and Peter A Lieberzeit[2]

[1] Department of Analytical Chemistry, University of Vienna, Währinger Strasse 38, 1090, Austria
E-mail: sadia.zafar.bajwa@univie.ac.at
[2] Department of Analytical Chemistry, University of Vienna, Währinger Strasse 38, 1090, Austria
E-mail: peter.lieberzeit@univie.ac.at

Metal ion imprinting technique is a recent focus of interest for synthesizing materials capable for precise, sensitive, and selective detection of metal ions [1-2]. Additionally, they constitute the smallest possible templates in molecular imprinting and, therefore allow in-depth assessment of interactions determining recognition. In the present study Cu^{2+} ions have been complexed with a polymerizable ligand, *N*-vinyl-2-pyrrolidone. This arrangement is further stabilized by suitable crosslinking monomer thus generating interaction sites based on the geometry of the respective complex within the polymer matrix for the re-inclusion of metal ions, after their removal. Materials are characterized by AT-IR and UV-VIS spectroscopy that support the presence of coordination bonds between the functional monomer and the analyte. Furthermore, a model is proposed based on these spectroscopic observations confirming binding via both the carbonyl functionality and the tertiary nitrogen atom of the N-vinyl-2-pyrrolidone. The sensor properties of materials have been studied with periodic microelectrode devices. The ion-imprinted polymer shows seven times more sensitivity to the presence of Cu2+ ions as compared to the respective non-imprinted one. The sensor signal is not only fast (ca. 1min.) but also reproducible within 4% of the original value. Polymer optimization plays an important role for recognition: a ratio of 2 parts of crosslinker to one part of functional monomer leads to an optimized signal of 745 µS. The sensor characteristics are found linear over a wide range of Cu^{2+} concentration (1×10^{-6} to 1×10^{-3} M) with 20 µM as the lower limit of detection. Additionally, 400 nm coating height of the imprinted material on the transducer provides optimal diffusion pathways for the re-adsoprtion of Cu^{2+} ions. The sensor layer prefers its own template by the factor of two in the presence of interfering bivalent ions of closer radii as Co^{2+}, Ni^{2+}, and Zn^{2+}, whereas for ions as Na^{+} having poor complexibility shows two times less sensitivity than Cu(II) ions. The sensor device exhibits the same quality of sensor signal in spiked natural water samples as with de-ionized water.

REFERENCES

[1] Latif, U., Mujahid, A., Afzal, A., Sikorski, R., Lieberzeit, P., Dickert, F., *"Dual and tetraelectrode QCMs using imprinted polymers as receptors for ions and neutral analytes",* Analytical and Bioanalytical Chemistry, 1-9 (2011)

[2] Bi, X., Lau, RJ., Yang, KL., *"Preparation of ion-imprinted silica gels functionalized with glycine, diglycine, and triglycine and their adsorption properties for copper ions"* Langmuir **23**, 8079-8086 (2007)

O17: Gas-Phase Electrophoretic Mobility Separation as a Tool for Sizing and Characterizing Nanoparticles

Angela Lehner[1], Victor U. Weiss[1], Martina Marchetti-Deschmann[1], Wladyslaw Szymanski[2] and Guenter Allmaier[1]

[1] Vienna University of Technology, Institute of Chemical Technologies and Analytics, Getreidemarkt 9/164IAC, 1060 Vienna, Austria,
E-mail: angela.lehner@tuwien.ac.at
[2] University of Vienna, Faculty of Physics, Boltzmanngasse 5, 1090 Vienna, Austria

Engineered nanoparticles (ENP) pose a new challenge to analytical chemists as they are considerably bigger (1-100 nm in at least one dimension resp. 1-1000 nm – no definition agreed upon yet [1]) than the usual atoms, molecules and complexes which most analytical instruments can handle in a confident manner.

The demand for robust methods of detecting and characterizing ENPs are exponentially growing as ENPs enter more and more sectors of our daily lives – just in the food sector 400 companies were estimated to be active in nanotechnologies research and development in 2010 [2] and mandatory labelling regulations of "nano" ingredients were adopted by the European Union in 2011 and are discussed in OECD countries currently [3].

Gas-Phase Electrophoretic Molecular Mobility Analysis (GEMMA) in combination with nano electrospray (nES) is a technique that can meet the needs of ENP characterization and allows number particle concentration determination [4] as well as monitoring even labile organic nanoparticles in food [5]. The basic concept of this technique will be presented briefly, before examples of organic (gelatine, liposomes, viruses and virus-like particles) as well as inorganic (silicon dioxide and silver) ENPs measured with nES GEMMA will be shown. For further characterization nES GEMMA can be combined with immuno detection, AFM (atomic force microscopy) and EM (electron microscopy) which will be described from the technology viewpoint and also some examples will be presented.

REFERENCES

[1] Lövenstam, G., Rauscher H., Roebben, G. Sokull Klüttgen B. Gibson N. Putaud J.-P., Stamm H., *"Considerations on a Definition of Nanomaterial for Regulatory Purposes",* Joint Research Center of the European Commission (JRC) Reference Report (2010)

[2] Kaiser, H., *"Nanotechnology in Food and Food Processing Worldwide 2003-2006-2010-2015"*, Helmut Kaiser Consulting, Tuebingen, Germany (2006)

[3] Gruère G.P., "Implications of nanotechnology growth in food and agriculture in OECD countries", Food Policy **37**, 191-198 (2012)

[4] Allmaier G, Maißer A., Laschober C., Messner P. Szymanski W. W., *"Parallel differential mobility analysis for electrostatic characterization and manipulation of nanoparticles and viruses",* Trends in Analytical Chemistry **30** (1), 123-132 (2011)

[5] Peters R., Ten Dam G., Bouwmeester H., Helsper H., Allmaier G., Kammer F. vd, Ramsch R., Solans C., Tomaniová M., Hajslova J., Weigel S., „Identification and characterization of organic nanoparticles in food", Trends Analytical Chemistry **30** (1), 100-112 (2011)

Acknowledgements:

The work leading to these results has received funding from the Austrian Science Foundation (Grant TRP29-N20) and European Union FP7/2007-2013 (grant n° 245162).

O18: Advanced Vibrational Spectroscopic Imaging of Human Tissue Micro Arrays Containing Cancer Tissue in Life Science

C. Pezzei[1*], J. D. Pallua[1*], G. Schaefer[2], V. Huck-Pezzei[1], L. K. Bittner[1], S. A. Schoenbichler[1], H. Klocker[2], G. Bartsch[2], G. K. Bonn[1] and C. W. Huck[1]

[1] Institute of Analytical Chemistry and Radiochemistry, Leopold-Franzens University, Innrain 52a, 6020 Innsbruck, Austria;
E-mail: Christian.W.Huck@uibk.ac.at
[2] Department of Urology, Medical University of Innsbruck, Anichstraße 35, 6020 Innsbruck, Austria

*First two authors contributed equally to this work

Among the many diseases affecting humans, cancer is a major public health challenge, being the second most common cause of death after cardio-vascular diseases. Diagnosis of cancer is based on clinical observation and imaging techniques. Various imaging technologies have been developed to complement the clinical and pathological examination of the original staging process of cancers [1].
Non-invasive radiological methods do not give an overview of the biochemical composition in order to correctly classify tumorous tissue or even detect suspicious areas. Biochemical processes during cancer development and progression are too complex to be totally elucidated by conventional techniques and the ideal imaging technique does not exist. [2]. The only reliable way to confirm cancer is the histopathological evaluation of tissue specimens using light microscopy (LM). Nonetheless this is an invasive method requiring patient´s tissue specimen (e.g. biopsies) and is a time consuming and sometimes subjective technique, with inter- and intra-observer discrepancy. The lack of reliable tools to a rapid diagnose cancer has led to a considerable amount of interest in the evolution of new techniques such as Fourier Transform Infrared (FTIR) imaging [3, 4], which has become an essential tool for detection, identification and characterization of the molecular components of biological processes. The acquisition of local molecular expression profiles while maintaining the topographic integrity of the tissue and avoiding time-consuming extraction, purification, and separation steps is a major advantage of this technique. This imaging method permits to obtain images of the spatial distribution of proteins, lipids, carbohydrates, cholesterols, nucleic acids, phospholipids, and small molecules within biological systems by in-situ analysis of tissue sections with high spatial resolution.
In our study, FTIR imaging combined with multivariate data analysis was used to collect and analyze IR spectra from formalin-fixed paraffin-embedded (FFPE) tissue micro arrays (TMAs) of prostate cancer tissue sections. The correlation of FTIR imaging to the morphological tissue features obtained by histological staining of the sections demonstrated that many histomorphological tissue patterns can be visualized in the colour images, which were created applying different algorithms. It is possible to distinguish between tumor and non tumor areas within prostate cancer tissue. For the interpretation of the vibrational spectroscopic results, FTIR-images were correlated with the histopathological information.

REFERENCES

[1] Luker, G.D., Special conference of the American Association for Cancer Research on molecular imaging in cancer. *Linking Biology, Function, and Clinical Applications in Vivo.* Cancer research, 2002. 62 (7): p. 2195.

[2] Glasspool, R. and T. Evans, *Clinical imaging of cancer metastasis*. European Journal of Cancer, 2000. 36 (13): p. 1661-1670.

[3] Bhargava, R., *Towards a practical Fourier transform infrared chemical imaging protocol for cancer histopathology.* Analytical and bioanalytical chemistry, 2007. 389 (4): p. 1155-1169.

[4] Pezzei, C., et al., *Characterization of normal and malignant prostate tissue by Fourier transform infrared microspectroscopy.* Mol. BioSyst., 2010. 6 (11): p. 2287-2295.

O19: Evaluation of hyperspectral imaging and classical vibrational spectroscopy for the quantification of furosemide polymorphs in ternary mixtures

S.A. Schönbichler *, L.K. Bittner *, C. Pezzei, G.K. Bonn, C.W. Huck

Institute of Analytical Chemistry and Radiochemistry
University of Innsbruck, Innrain 52a, 6020 Innsbruck, Austria
E-mail: Christian.W.Huck@uibk.ac.at

*Both authors contributed equally to this work

Quantification methods for ternary mixtures of polymorphic forms I, II and III of furosemide were developed using Raman, near-infrared spectroscopy (NIRS), fourier transform mid-infrared spectroscopy in attenuated total reflection mode (FTIR-ATR) and near-infrared hyperspectral imaging in combination with multivariate data analysis. Powder mixtures were prepared according a calculated design of experiment (DOE). The identity and the purity of the polymorphs were confirmed by powder x-ray diffraction (PXRD). For all methods partial least squares regression (PLSR) based calibration models were developed and quality parameters such as squared regression coefficients (R^2) and standard error of prediction (SEP) were compared. Different pretreatments were systematically carried out and evaluated. For hyperspectral images each data point was predicted and displayed quantitatively to ensure blending homogeneity. All methods except FTIR-ATR are suitable for quantification of furosemide polymorphs in ternary mixtures and even the imaging mode with lower spectra quality (e.g. lowest signal noise ratio (SNR)) delivered satisfactory calibrations. Due to pressure instability of form II, FTIR-ATR cannot be used for this purpose. This study is an all-embracing comparison of vibrational spectroscopic methods for the quantification of polymorphs using the example of furosemide. Advantages and disadvantages of the different spectroscopic and chemometric methods are demonstrated and critically discussed in the proposed presentation.

REFERENCES

[1] Braun, D.E., Maas, S.G., Zencirci, N., Langes, C., Urbanetz, N.A. and Griesser, U.J., "*Simultaneous quantitative analysis of ternary mixtures of d-mannitol polymorphs by FT-Raman spectroscopy and multivariate calibration models*", International Journal of Pharmaceutics, **385**(1-2): 29-36 (2010)

[2] Heinz, A., Savolainen, M., Rades, T. and Strachan, C.J., "*Quantifying ternary mixtures of different solid-state forms of indomethacin by Raman and near-infrared spectroscopy*", European Journal of Pharmaceutical Sciences, **32**(3): 182-192 (2007)

[3] Kolomiets, O., Hoffmann, U., Geladi, P. and Siesler, H., "*Quantitative Determination of Pharmaceutical Drug Formulations by Near-Infrared Spectroscopic Imaging*", Applied Spectroscopy, **62**(11): 1200-1208 (2008)

[4] Matsuda, Y. and Tatsumi, E., "*Physicochemical characterization of furosemide modifications*", International Journal of Pharmaceutics, **60**(1): 11-26 (1990)

Acknowledgements:

The authors like to thank Ulrich Griesser and Christoph Langes for carrying out the PXRD measurements.

O20: HILIC: A systematic column characterization

Schuster G[1].*, Lindner W[1].

[1] University of Vienna, Vienna, Austria,
E-mail: georg.schuster@univie.ac.at

Hydrophilic interaction liquid chromatography (HILIC) has become an established and alternative chromatography mode during method development, due to its orthogonal retention behavior to the still more popular reversed-phase (RP) mode.

Although, good results can be achieved, this method is still not as straight forward as conventional RP. A reason is the vast diversity of column materials available on the market. At first, HILIC was performed on bare silica packings. However, they now span from zwitterionic sulfobetain and phosphocholin type- to hydroxyl-, amide-, and urea- functionalized materials. Originally, a partition mechanism between a water rich hydro-organic stagnant liquid phase being supported by a polar stationary phase and an organic rich mobile phase was proclaimed to facilitate retention. However, due to the different type of modifications, observed selectivities influenced by adsorption processes lead to a “mixed mode” retention mechanism. Publications conclude that multiple screening of different stationary and mobile phase types are crucial during method development [1-3].

For this contribution we screened a set of 20 HILIC columns comprising neutral, basic, acidic and zwitterionic surface modifications. Homemade packing materials (with well-known chemistry) were compared to commercially available columns (with often undefined ligand structures and silica materials). A generic test set (e.g. acidic-, basic-, neutral-, zwitterionic-compounds, xanthines, nucleobases, nucleosides) was applied. Three different mobile phases ACN:H_2O (90:10; v/v) + 10 mM buffer (pH 3, 5 and 8) should further evaluate the pH dependency of different phase chemistries. The evaluation is carried out using multivariate statistical approaches to compare achieved retention profiles.

We hope that this observation leads to a more straight forward method development, discharging trial-and-error approaches under HILIC conditions and help choosing a sufficient set of HILIC columns to span a wide range in selectivity.

REFERENCES

[1] Jandera P., *J.Sep.Sci* **(2008)**, doi: 10.1002/jssc.20080051

[2] Fountain, K.J., et al., *J.Sep.Sci* **(2010)**, doi: 10.1002/jssc.200900660

[3] McCalley D.V., *J.Chromatogr. A* **(2010)**, doi:10.1016/j.chroma.2010.03.011

O21: NOVEL AMINOPHOSPHONATE MULTIMODAL SELECTORS FOR LIQUID CHROMATOGRAPHY BASED ON UGI-MULTICOMPONENT REACTION

Gargano A[1].*, Lindner W[1]., Lämmerhofer M[2].

[1] University of Vienna, Vienna, Austria;
E-mail: andrea.gargano@univie.ac.at
[2] University of Tuebingen, Tuebingen, Germany

In the present work a novel use of the Ugi multicomponent reaction (MCR) to generate zwitterionic chromatographic selectors for reverse phase (RP), RP/zwitterionic ion exchange and hydrophilic interaction liquid chromatography (HILIC) is described. Aminophosphonate zwitterionic chromatographic molecules were synthesized adopting a single one pot microwave assisted three-component UGI-MCR synthesis [1] and after purification were immobilized by thiol click chemistry on silica beads. Chromatographic characteristics of these stationary phases were evaluated comparatively to the structurally related commercially available ZIC-HILIC and phospho-ZIC HILIC columns. Interestingly multimodal separation capabilities were found for the novel selectors (i.e. columns can be operated both in HILIC and in RP mode with good selectivity and efficiency), characteristic not present for sulphobetain and phosphobetain type ZIC-HILIC columns.

Moreover, the adopted synthetic approach offer the capability to generate chemical diversity simply by the variation of the starting aldehyde, aminophosphonic acid and or isonitrile components. This unique characteristic offers great possibility for the design of novel selectors for mixed mode chromatography like RP/ZWIX, HILIC, affinity and chiral chromatography.

REFERENCES

[1] A. Dömling, I. Ugi, *Angewandte Chemie International Edition* **2000**, *39*, 3168.

Acknowledgements:

This work was financially supported by the University of Vienna through the doctoral program, “Initiativkolleg Functional Molecules” (IK I041−N)

O22: Identification and quantitation of hindered amine light stabilizers (HALS) by HPLC/MS or direct MS/MS

Michael Reisinger[1], Susanne Beißmann[1], Wolfgang Buchberger[1] and Christian Klampfl[1]

[1] Johannes Kepler-University Linz, Altenberger Straße 69, A-4040 Linz/Austria
E-mail: michael.reisinger_1@jku.at

Polymers, such as polyolefines, are getting an increased importance due to their wide range of applications. For the extension of polymer lifetime, different kinds of stabilizers are required to protect the materials from environmental impacts. To ensure long time stabilization, hindered amine light stabilizers (HALS) are the most common type of UV-stabilizers which are used in polyolefines. HALS are monomeric or oligomeric substances of higher molecular weight that can interfere with the formation of radicals caused by UV-radiation and they also get regenerated within a cyclic reaction process.

Analytical methods published so far for HALS include pyrolysis-GC/MS [1], HPLC-UV [2] and photometric procedures, whereby the latter can only quantify the sum of HALS. Reliable HPLC methods are not yet available to separate all oligomers of HALS.

In the present work we want to demonstrate the separation and the quantitation of different hindered amine light stabilizers. The separation is done with a polymer column at pH values above 11, where normal reversed phased columns cannot be used. The separated analytes were introduced into an Agilent 6510 Q-TOF mass spectrometer using electrospray ionization (ESI) in the positive mode. The main signals can be explicitly assigned to the molecular formula of the monomers and also oligomers. Alternatively, a flow injection technique with MS/MS detection was developed and compared with the HPLC method. Advantages and disadvantages of each approach will be discussed within this presentation.

REFERENCES

[1] L. Coulier, E.R. Kaal, M. Tienstra, Th. Hankemeier, *J.Chromatogr. A*, 993 (2003) 137-142

[2] A. Farajzadeh, S.G. Eskandar, A. Ranji, E. Feyz, *Microchim Acta* (2007) 159; 363-369

O23: Analytical characterisation (HPLC-MS) of biomass pretreated by the “steam explosion”-process

Thomas Schmid[1], Wolfgang Buchberger[1] and Markus Himmelsbach[1]

[1]Johannes Kepler University Linz, Altenberger Straße 69, A-4040 Linz/Austria
E-mail: Thomas.Schmid@jku.at

Plant biomass can be used as substrate for the generation of energy. A possibility for its utilization is the conversion into other energy carriers such as ethanol or methane, which is achieved by fermentation with microorganisms. Lignocellulosic materials such as wood or straw are an especially interesting class of substrates as they often appear as agricultural by- or waste-products. However, due to their structure an initial pre-treatment step of lignocellulosic biomass is necessary in order to make the substrate hydrolytically degradable. A widely applied method is the “steam explosion”-process, where the substrate is treated with saturated steam under pressure, followed by a sudden expansion after a defined period of time. Beside the desired effects on the substrate, various degradation products are formed, which are known to inhibit the subsequent fermentation.

Analytical investigations of biomass degradation products include GC-MS after derivatization [1-2] as well as RP-HPLC with UV-detection [3].

In the present work a HPLC-method coupled with MS-detection has been developed for the determination of potential fermentation inhibitors. The analytes have been ionized using electrospray ionization (ESI) in the positive mode and detected with an Agilent 6510 Q-TOF. Four lignocellulosic biomass substrates pretreated by the “steam explosion”-process at different conditions concerning applied pressure and holding time have been investigated. Special attention was paid to the correlation between strength of pretreatment and concentration of inhibitors.

REFERENCES

[1] Luo, C., Brink, D.L., Blanch H.W., *“Identification of potential fermentation inhibitors in conversion of hybrid poplar hydrolyzate to ethanol”*, Biomass and Bioenergy **22** (2), 125-138 (2002)

[2] Klinke, H.B., Ahring, B.K., Schmidt, A.S., Thomsen, A.B., *“Characterization of degradation products from alkaline wet oxidation of wheat straw”*, Bioresource Technology **82** (1), 15-26 (2002)

[3] Chen, S.-F., Mowery, R.A., Castleberry, V.A., van Walsum, G.P., Chambliss, C.K., *“High-performance liquid chromatography method for simultaneous determination of aliphatic acid, aromatic acid and neutral degradation products in biomass pretreatment hydrolysates”*, Journal of Chromatography A **1104** (1-2), 54-61 (2006)

O24: ANALYSIS OF THE PROTEOME OF MONOCYTIC AND DENDRITIC CELLS

Melanie Rothauer[1], Lisa Weilnböck[1], Jutta Horejs-Höck[2], and Christian C. Huber[1]

[1] Division of Chemistry and Bioanalytics and [2] Division of Immunology, Department of Molecular Biology, University of Salzburg, Hellbrunner Str. 34, 5020 Salzburg, Austria,
E-mail: melanie.rothauer@stud.sbg.ac.at

Dendritic cells (DCs) are one of the key figures in the immune system as they play an important role in the activation of adaptive immune response. In due consequence, the analysis of the secretome and proteome of DCs is one of the main focuses of clinical proteomics research. Proteome analysis based on mass spectrometry enables the identification of important proteins which are involved in the communication of DCs with other cells. In this study the analysis of the DCs is accomplished by shotgun and targeted proteomics using LC-MS.

As the amount of cells available from healthy donors is relatively low, the monocytic leukaemia cell-line THP-1 was used as model system for DCs. In cell culture, immune cells release proteins into the medium, which usually contains Fetal Calf Serum (FCS) to enable growth of the cells. Because of the high protein concentration in the serum, mass spectrometric analysis of the supernatant and therefore of important signalling molecules, becomes infeasible. To overcome this problem, we decided on inhibiting the secretion of DCs by using different inhibitors that influence specific secretion events. The effects of the inhibitors on monocyte-derived dendritic cells (moDCs) and THP-1 cells was evaluated by cytokine enzyme-linked immunosorbent assays (ELISAs) with the cytokines Interleukin 1beta, Tumor Necrosis Factor alpha and Interleukin 12. To confirm the presence of the cytokines in the cytosol, antibody affinity chromatography selective for the three cytokines was performed.

For the extraction of the proteins from cell lysate, denaturation, reduction, alkylation and digestion with trypsin were performed. The separation of the resulting peptides was achieved by ion-pair reversed-phase high-performance liquid chromatography (HPLC) using a 150 x 0.20 mm i.d. monolithic poly(styrene-divinylbenzene) (PS-DVB) column, a flow rate of 1 µl/min and a linear gradient of 0 – 40 % acetonitrile in 0.05 % aqueous trifluoroacetic acid in 300 min at 55 °C. The IP-RP-HPLC system was directly hyphenated to LTQ-Orbitrap XL mass spectrometry using nano-electrospray ionization. The peptides were identified using tandem mass spectrometry following collision induced dissociation (CID).

We were able to approve the inhibition of the secretion by using ELISA with the cytokines IL 12 and TNF alpha with the inhibitor Brefeldin A. IL 1beta showed no inhibition because it uses a non-classical secretion pathway without the Endoplasmatic Reticulum and the Golgi apparatus. On this account IL 1beta is a clear evidence and control for the integrity and functionality of the cells in presence of the inhibitor.

Finally, the proteome of dendritic cell lysates treated with Brefeldin A was analysed in three replicate high-resolution peptide separations hyphenated to LTQ-Orbitrap mass spectrometry and applying exclusion lists in order to maximize the identification rate and avoid the repetitive identification of the same peptides. The identified proteins and their gene ontology facilitated useful insights into the functional state and the active biological pathways of dendritic cells, which are essential for the dissemination of the immune response.

O25: LC-HRMS/MS based approach for the screening of microbial iron-containing metabolites (siderophores)

Sylvia M. Lehner[1], Nora K. N. Neumann[1], Lea Atanasova[2], Rudolf Krska[1], Marc Lemmens[3], Irina S. Druzhinina[2], Rainer Schuhmacher[1]

[1] Center for Analytical Chemistry, Department for Agrobiotechnology (IFA-Tulln), University of Natural Resources and Life Sciences Vienna, Konrad Lorenz Str. 20, 3430 Tulln, Austria,
E-mail: sylvia.lehner@boku.ac.at
[2] Institute of Chemical Engineering, Vienna University of Technology, Gumpendorfer Str. 1a, 1060 Vienna, Austria
[3] Institute for Biotechnology in Plant Production, Department for Agrobiotechnology (IFA-Tulln), University of Natural Resources and Life Sciences Vienna, Konrad Lorenz Str. 20, 3430 Tulln, Austria

Siderophores (from the Greek: sideros “iron”, phorein “to carry sth.”) are ferric-iron-chelating compounds with a molecular mass of approx. 500-1500 Da. Due to low solubility of iron under environmental conditions, plants and microbes produce and secrete Fe-chelating metabolites, i.e. siderophores into the soil in order to solubilize and thereby satisfy their demand of iron [1].

The present study aimed at the establishment of a screening strategy for siderophores using liquid chromatography – high-resolution tandem mass spectrometry (LC-HRMS/MS) on an LTQ Orbitrap XL. Therefore, a systematic screening approach for iron-containing metabolites in biological samples was established. In this respect, LC-MS full scan mass spectra were recorded from m/z 200 to m/z 2000 and a data evaluation tool was implemented in python to search for the characteristic iron isotopic pattern of ^{54}Fe:^{56}Fe. Moreover, concurrent peak shapes of the respective extracted ion chromatograms (EICs) were verified. Corresponding hits were queried against an in-house siderophore library containing 525 fungal and bacterial siderophores. Further criteria for the confirmation of siderophores included the specific UV/VIS absorption at 420-450 nm as well as characteristic mass shifts in MS/MS fragment spectra.

The described screening approach was applied to investigate various species of the filamentous fungus *Trichoderma*. The findings include known, fungal siderophores such as dimerum acid, coprogen, fusigen and ferricrocin. Additionally, a variety of to date unknown putative siderophores with masses ranging from 500-1000 Da were found. The results were correlated with the phylogenetic relationship of the strains under investigation as well as the recently published genomes of three of the investigated *Trichoderma* strains.

REFERENCES

[1] Hider R.C. and Kong X., “Chemistry and biology of siderophores”, Natural Product Reports **27**, 637-657 (2010)

Acknowledgements:

The Federal Country Lower Austria and the European Regional Development Fund (ERDF) of the European Union is acknowledged for financial support (Grant Number GZ WST3-T-95/001-2006).

O26: GC-MS Based Metabolomics to Study *Fusarium* Head Blight

D.Schöfbeck[1], N. Neumann[1], B. Kluger[1], M. Lemmens[2], G. Adam[3], G. Wiesenberger[3], R. Krska[1], R. Schuhmacher[1]

[1] Center for Analytical Chemistry, [2] Institute for Biotechnology in Plant Production, Department IFA-Tulln, University of Natural Resources and Life Sciences Vienna, Konrad Lorenz Straße 20, 3430 Tulln
E-mail: denise.schoefbeck@boku.ac.at
[3] Department of Applied Genetics and Cell Biology, University of Natural Resources and Life Sciences Vienna, Konrad Lorenz Straße 24, 3430 Tulln

Metabolomics aims at the comprehensive, non-targeted analytical determination of all metabolites (metabolome) of a biological system [1]. Due to the high complexity and high dynamic range of the metabolome this is a very challenging task and requires the use of various analytical techniques. We have developed a GC-MS based methodology for the targeted as well as the non-targeted profiling of volatiles and polar non-volatile metabolites.

The presented study was carried out as part of an interdisciplinary research project, which aims at the investigation of fungal virulence and plant resistance in the *Fusarium* Head Blight disease (FHB). Both, fungal cultures of *F. graminearum* and *Fusarium* infected and non-infected wheat ears were analysed by GC-MS. Fungal cultures of *F. graminearum* as well as *Fusarium* infected and non-infected wheat ears were analysed by GC-MS. Volatile profiles were determined using headspace solid phase microextraction (HS SPME), while small polar metabolites were measured after a two step derivatisation employing methoxyamine (MOX) and N-methyl-N-trimethylsilyl trifluoroacetamide (MSTFA). GC-MS chromatograms were deconvolved and further processed with MetaboliteDetector [2].

Pilot experiments revealed that *F. graminearum* PH-1 is capable of producing complex mixtures of volatile metabolites, which are mainly dominated by bioactive sesquiterpenes and amino-acid derived metabolites, which are probably involved in the interaction with the host plant during/upon infection. Moreover, GC-MS analysis of wheat ears resulted in the detection of more than hundred different volatile and non-volatile metabolites, many of those were significantly affected in the presence of the fungus (e.g. different alkanes, aldehydes and ketones). In this contribution we will present in detail the GC-MS results of our latest metabolomics experiment with the goal to identify wheat metabolites, which are closely linked to defined genetic resistance markers in the wheat genome.

REFERENCES

[1] Dunn W.B., Ellis D.I., „*Metabolomics: Current analytical platforms and methodologies*", Trends in Analytical Chemistry **24** (4), 285-294 (2005)

[2] Hiller K. et al., *"MetaboliteDetector: Comprehensive Analysis Tool for Targeted and Nontargeted GC/MS Based Metabolome Analysis"*, Analytical Chemistry **81** (9), 3429-3439 (2009)

Acknowledgements:

The authors thank the Austrian Science Fund (FWF) for financial support of the project F37 „SFB *Fusarium*".

O27: *In vivo* ^{13}C labelling for the study of metabolite profiles of different strains of *Fusarium graminearum* by LC/MS

Bernhard Kluger[1], Christoph Bueschl[1], Stefan Bödi[2], Joseph Strauss[2], Rudolf Krska[1] and Rainer Schuhmacher[1]

[1] Center for Analytical Chemistry, Department for Agrobiotechnology IFA-Tulln, University of Natural Resources and Life Sciences Vienna, 3430 Tulln, Austria,
E-mail: bernhard.kluger@boku.ac.at
[2] Fungal Genomics Unit (UFT-Tulln), University of Natural Resources and Life Sciences Vienna, Konrad Lorenz Straße 24, A-3430 Tulln, Austria

Non-targeted metabolomics based on ESI-LC/MS is a major challenge due to the fact that full scan spectra contain a lot of non-metabolite related background signal in addition to mass peaks originating from true metabolites. In this study we made use of *in vivo* stable isotopic labelling [1] of the plant pathogenic fungus *F. graminearum* for the unambiguous assignment and differential comparison of metabolites of true biological origin.
To this end, spores of *F. graminearum* PH-1 and two epigenetic mutants Δhep1 and Δccl1 were cultivated under identical conditions. The Δ*Hep1* mutant is deficient in the production of heterochromatin protein 1 which stabilises heterochromatin structure by binding to Lys9 of histone 3, whereas the knock out mutant Δ*ccl1* is deficient in the production of a methyltransferase for the methylation of the Lys4 residue. Both mutations can be expected to cause substantial changes in the chromatin structure thereby altering the formation of secondary metabolites compared to the wildtype PH-1. To test this hypothesis, all three strains were cultivated on the same nutrition media (Fusarium minimal medium) containing either ^{12}C or $^{13}C_6$ glucose as sole carbon source. A 1+1 mixture of both culture filtrates (non-labelled and fully labelled) was prepared and analysed by LC/MS analysis with the LTQ-Orbitrap XL mass spectrometer in both positive and negative ionisation mode. For each detected metabolite the obtained high resolution mass spectra simultaneously contained mass peaks of both non-labelled and corresponding fully labelled isotopologues. The resulting pattern of the isotopologues can only be observed for true biological metabolites and was automatically detected by the in house developed algorithm MetExtract [2].
As a result, a list of true biological metabolites originating from the fungi was created which contained accurate masses, adduct ions and number of carbon atoms allowing a comparison of the metabolite profile. For these assigned metabolites data were further evaluated with the aim to identify substances differentially expressed by the epigenetically different *F. graminearum* strains.

REFERENCES

[1] Giavalisco P., Hummel J., Lisec J., Alvaro C.I., Catchpole G., Willmitzer L., *"High-Resolution Direct Infusion-Based Mass Spectrometry in Combination with Whole ^{13}C Metabolome Isotope Labeling Allows Unambiguous Assignment of Chemical Sum Formulas",* Analytical Chemistry **80**, 9417–9425 (2008)

[2] Bueschl C., Kluger B., Berthiller F., Lirk G., Winkler S., Krska, R., Schuhmacher R., *" MetExtract: A new software tool for the automated comprehensive extraction of metabolite-derived LC/MS signals in metabolomics researc*h", Bioinformatics **28** (5), 736-738 (2012)

Acknowledgements:

The authors thank the Austrian Science Fund (FWF) for financial support of the project F37 „SFB *Fusarium*".

O28: Pentahydroxyscirpene – detection, isolation, structure elucidation and toxicity assessment of a new mycotoxin

Elisabeth Varga[1], Philipp Fruhmann[2], Christian Hametner[2], Gerlinde Wiesenberger[3], Hannes Mikula[2], Rudolf Krska[1], Gerhard Adam[3], Marc Lemmens[4], Johannes Fröhlich[2] and Franz Berthiller[1]

[1] University of Natural Resources and Life Sciences, Vienna (BOKU), Dept. for Agrobiotechnology (IFA-Tulln), Center for Analytical Chemistry and Christian Doppler Laboratory for Mycotoxin Metabolism, Konrad Lorenz Str. 20, A-3430 Tulln,
E-mail: elisabeth.varga@boku.ac.at
[2] Institute of Applied Synthetic Chemistry, Vienna University of Technology, Getreidemarkt 9/163, A-1060 Vienna
[3] BOKU, Dept. of Applied Genetics and Cell Biology, Konrad-Lorenz-Str. 24, A-3430 Tulln
[4] BOKU, IFA-Tulln, Institute of Biotechnology in Plant Production, Konrad Lorenz Str. 20, A-3430 Tulln

Trichothecenes are an important class of mycotoxins and are characterised by a double bond between C9 and C10 and an epoxy ring at the C12-C13 position. More than 200 different subtypes are already characterized and described in literature [1]. However, due to the characteristic backbone structure which provides an ideal scaffold for different functional groups, numerous yet unidentified compounds might exist.

A routine purity check of a crude nivalenol (NIV) sample via NMR, revealed a substantial amount of a structurally closely related compound. Since the polarity was slightly different from that of NIV both substances were purified via normal phase - liquid chromatography. Nearly 15 mg (~20 w% of the sample) of the white powdered unknown substance were obtained. For structure elucidation several 1D- and 2D-NMR experiments including ^{1}H-, ^{13}C-, HH-COSY, HC-HSQC and HC-HMBC were performed and resulted in the chemical structure of pentahydroxyscirpene (PHS).

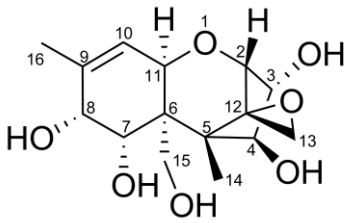

3α,4β,7α,8α,15-Pentahydroxy-scirp-9-ene (PHS)

The production of NIV and PHS was repeated on rice inoculated with the same *Fusarium* strain for several weeks. The purpose of this experiment was to confirm the origin of the compound as well as to ensure that it is not an artefact of purification or degradation product of NIV. After three weeks of incubation average concentrations of a biological triplicate of 1.38 ± 0.07 g/kg for NIV and 0.32 ± 0.04 g/kg for PHS were observed by LC-MS/MS measurements.

Toxicity of PHS was evaluated with an *in vitro* toxicity test, based on the inhibition of protein synthesis by trichothecenes. The translation of firefly luciferase was suppressed to 50% (IC_{50}) at 0.5 µM NIV and 1.0 µM PHS. The potency of PHS to inhibit protein biosynthesis is very similar to that of the known Fusarium mycotoxin deoxynivalenol (IC_{50} of 1.0 µm).

REFERENCES

[1] Grove, J.F., *"The Trichothecenes and Their Biosynthesis"*, Progress in the Chemistry of Organic Natural Products **88**, 63-130 (2007)

Acknowledgements:

The authors thank the FWF (project SFB-Fusarium) and the Federal Ministry of Economy, Family and Youth, the National Foundation for Research, Technology and Development. Furthermore, we want to acknowledge the financial support of the graduate school programme Applied Bioscience Technology of the Vienna University of Technology.

O29: LC-MS based method development for metabolomic analysis in human cell cultures

Ines C. Forstenlehner[1], Volker Neu[1] and Christian G. Huber[1]

[1] Division of Chemistry and Bioanalytics, Department of Molecular Biology, University of Salzburg, Hellbrunner Str. 34, 5020-Salzburg, Austria.
E-mail: ineschristina.forstenlehner@sbg.ac.at

The human metabolome consists of an enormous number of metabolites, such as organic acids, amino acids, and lipids. Mass spectrometry-based metabolomics is a dramatically developing field that aims to do global metabolic fingerprinting and quantitative metabolite profiling, which allows comparative studies of metabolic fingerprint patterns providing information about changes in metabolic composition. A precise analysis of changes in concentration of metabolites is promising to provide information about basic biological mechanisms and reactions that take place in response to environmental and genetic modifications. Therefore comparative metabolome analysis is able to predict poor state of health in humans such as intoxication, disease, and genetic alterations at a very early stage.

The object of the study was to develop a liquid chromatography-mass spectrometry (LC-MS) based method to analyse human metabolomic cell extracts. This raised the problems of high chemical diversity and a wide concentration range of metabolites. Different stationary phases were pretested by LC-ESI-LTQ Orbitrap XL-MS using 0.1 % formic acid and 0.05 % trifluoroacetic acid as additives in both positive and negative ion mode. During the optimization process of the LC-MS method special focus was laid on influential factors of the ionization process, such as mobile phase additives and their concentrations and parameters concerning the LC-MS-interface. Furthermore, changes in retention mechanisms in both the Discovery HS F5, a pentafluorophenyl phase, and the Synergi Fusion-RP, a polar embedded C18 phase were modified by using different mobile phase additives. Additionally, we aimed to point out the advantages of LC-MS over direct infusion-mass spectrometry (DI-MS). Equally spaced serial dilution of a metabolite standard was conducted and measured by DI-MS and compared to LC-MS results. In order to prove that this method is also applicable to real samples, we conducted the measurements with metabolite cell extracts obtained from the tumor cell line Panc1.

The most effective measurements were done by using the Discovery HS F5 with eluents H_2O + 0.1 % formic acid, and acetonitrile + 0.1 % formic acid although the performance was comparable to the Synergi Fusion-RP. Both showed distinct and sharp peak shapes in satisfying intensities that were most spread over the whole chromatogram. By applying this optimized LC-MS method using the Discovery HS F5 as stationary phase, we reached an average peak width at base of 0.41 min and the widest spreading of metabolite retention times over the whole run. Above all we were able to detect all 27 model metabolites. 22 were detected by using negative ionization mode and 18 were detected in positive mode. The comparison of the direct infusion approach to the LC-MS measurements showed that, although the DI-MS was less time consuming, problematic issues such as ion suppression and other matrix effects could only be reduced by LC-MS. Furthermore, the separation of isomers with LC-MS was successfully demonstrated.

Acknowledgements:

The Panc1 cells were kindly provided by Andrea Loipetzberger, MSc, from the Division of Molecular Tumor Biology, Department of Molecular Biology, University of Salzburg, Austria. We also thank Lisa Weilnböck, MSc, from the Division of Chemistry and Bioanalytics, Department of Molecular Biology, University of Salzburg, Austria, for her support with the real sample preparation.

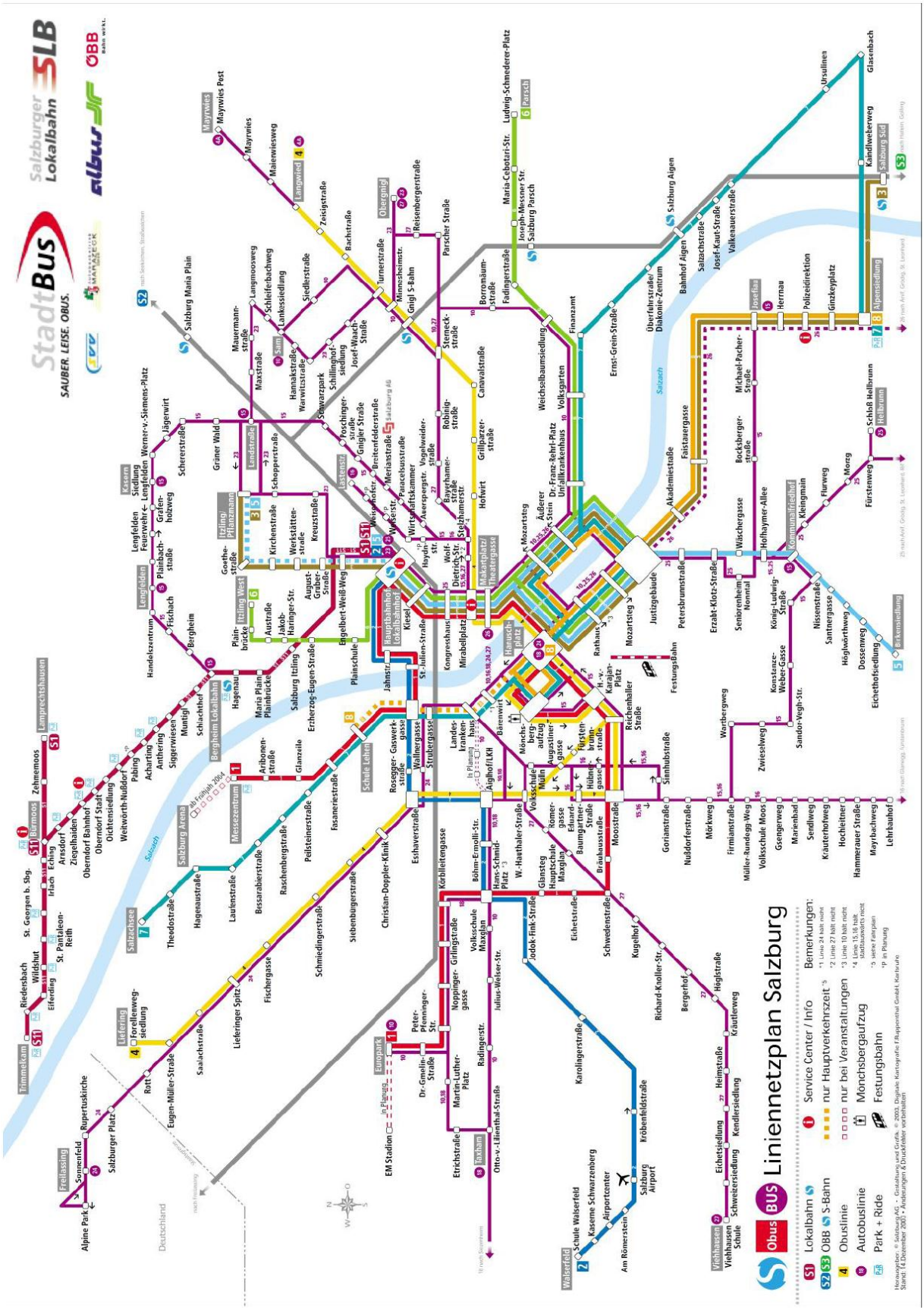
StadtBus
SAUBER. LEISE. OBUS.
Salzburger Lokalbahn SLB
ÖBB
albus
Liniennetzplan Salzburg
Obus BUS
S1 Lokalbahn
S2 S3 ÖBB S-Bahn
4 Obuslinie
8 Autobuslinie
P+R Park + Ride
Service Center / Info
nur Hauptverkehrszeit
nur bei Veranstaltungen
Mönchsbergaufzug
Festungbahn
Bemerkungen:
Deutschland
Salzach
Alpine Park
Salzburger Platz
Rupertuskirche
Sonnenfeld
Freilassing
Trimmelkam
Riedersbach
Wildshut
Eiferding
St. Georgen b. Sbg.
Irlach
Eching
Arnsdorf
Ziegelhaiden
Oberndorf Bahnhof
Oberndorf Stadt
Oichtensiedlung
Weitwirth-Nußdorf
Pabing
Achathing
Anthering
Siggerwiesen
Muntigl
Schlachthof
Zehnmoos
Bürmoos
Lamprechtshausen
Handelszentrum
Fischach
Borgheim
Bergheim Lokalbahn
Hagenau
Maria Plain Plainbrücke
Arbonenstraße
Glanzeile
Messezentrum
Salzburg Arena
Ab Frühjahr 2014
Theodorstraße
Hageaustraße
Lauferstraße
Bessarabierstraße
Raschenbergstraße
Peilsteinerstraße
Fasaneriestraße
Siebenbürgerstraße
Schmiedingerstraße
Fischergasse
Lieferinger Spitz
Saalachstraße
Eugen-Müller-Straße
Lufpring
Forellenweg-siedlung
Salzachsee
Salzachsee
Christian-Doppler-Klinik
Eshavarstraße
Rosegger-straße
Gaswerk-gasse
Wallnergasse
Strubergasse
Schule Lehen
Plainschule
Engelbert-Weiß-Weg
Jakob-Haringer-Str.
Austraße
Plain-brücke
Itzling West
Goethe-straße
Kirchenstraße
Werkstätten-straße
Kreuzstraße
Itzling Pflanzham
Landstraße
Schopperstraße
Grüner Wald
Schererstraße
Jägerwirt
Werner-v.-Siemens-Platz
Kasern Siedlung
Lengfelden Feuerwehr
Lengfelden
Grafen-holzweg
Plainbach-straße
Lengfelden
Salzburg Itzling
Ernst-Thun-Straße
Jahnstr.
St.-Julien-Straße
Hauptbahnhof Lokalbahnhof
Kiesel
Kongresshaus
Mirabellplatz
Hanuschplatz
Theatergasse
Hofwirt
Mozartsteg
Auerspergstr.
Bayerhamer-straße
Stelzhamerstr.
Wirtschaftskammer
Vogelweider-straße
Robinig-straße
Canavalstraße
Grillparzer-straße
Dr.-Franz-Rehrl-Platz
Unfallkrankenhaus
Auberer Stein
Weichselbaumsiedlung
Volksgarten
Finanzamt
Ernst-Grein-Straße
Überfuhrstraße
Diakonie-Zentrum
Salzburg Aigen
Bahnhof Aigen
Akademiestraße
Faistauergasse
Salzachstraße
Josef-Kaut-Straße
Valkenauerstraße
Ursulinen
Glasenbach
Kandlweberweg
Salzburg Süd
Alpensiedlung
Ginzkeyplatz
Polizeidirektion
Josefiau
Herrnau
Michael-Pacher-Straße
Backsberger-straße
Wäschergasse
Hofhaymer-Allee
Kommunalfriedhof
Kleingmain
Flurweg
Morzg
Fürstenweg
Schloß Hellbrunn
Hellbrunn
Birkensiedlung
Nissenstraße
Santnergasse
Högl-wörthweg
Dossenweg
Eichethofsiedlung
Königin-Ludwig-Straße
Senioren-heim Nonntal
Erzabt-Klotz-Straße
Petersbrunnstraße
Juvigebäude
Festungsbahn
Mozartsteg
Rathaus
H. v. Karajan-Platz
Reichenhaller Straße
Sinnhubstraße
Wartbergweg
Sandor-Vegh-Str.
Konstanze-Weber-Gasse
Zwiesselweg
Nußdorferstraße
Mörkweg
Goriantraße
Firmianstraße
Müller-Rundegg-Weg
Volksschule Moos
Gsengerweg
Marienbad
Sendlweg
Kräuterhofweg
Hocheitner
Hammerauer Straße
Maybachweg
Lehrbauhof
Dr.-Franz-Rehrl-Platz
Weichselbaumsiedlung
Joseph-Messner Str.
Salzburg Parsch
Ludwig-Schmederer-Platz
Parsch
Maria-Cebotari-Str.
Fadingerstraße
Borromäum-straße
Parscher Straße
Steineck-straße
Reisenbergerstraße
Gnigl S-Bahn
Mönnsheimstr.
Turnerstraße
Obergnigl
Josef-Wiach-Straße
Schillinghof-siedlung
Schwarzpark
Hannakstraße
Warwitzstraße
Siedlerstraße
Zeisigstraße
Bachstraße
Langwied
Maierwieswg
Maxstraße
Mauermann-straße
Schleiferbachweg
Langmoosweg
Lanksiedlung
Zum
Maywies
Maywies Post
Salzburg Maria Plain
Hasenauerstraße
Hasenauerstraße
Gnigler Straße
Poschinger-straße
Breitenfelderstraße
Merianstraße
Panaceibusstraße
Lastenstr.
Weißhofer
Wiesbauerstr.
Haydn-str.
Wolf-Dietrich-Str.
Salzburg 46
Hasenauerstraße
Hasenauerstraße
Obus
Linie 1
Linie 2
Linie 3
Linie 4
Linie 5
Linie 6
Linie 7
Linie 8
Linie 9
Linie 10
Linie 15
Linie 16
Linie 17
Linie 18
Linie 19
Linie 20
Linie 24
Linie 25
Linie 26
Linie 27
Linie 28
Linie 29
Linie 45
Linie 49
Linie 51
Linie 55
Linie 60
Linie 66
Linie 88
Linie 99
Linie 150
Linie 151
Linie 170
Linie 180
Linie 181
Linie 182
Linie 183
Linie 184
Linie 185
Linie 186
Linie 187
Linie 188
Linie 189
Linie 190
Linie 191
Linie 192
Linie 193
Linie 194
Linie 195
Linie 196
Linie 197
Linie 198
Linie 199
Linie 200
Linie 201
Linie 202
Linie 203
Linie 204
Linie 205
Linie 206
Linie 207
Linie 208
Linie 209
Linie 210
Linie 211
Linie 212
Linie 213
Linie 214
Linie 215
Linie 216
Linie 217
Linie 218
Linie 219
Linie 220
Linie 221
Linie 222
Linie 223
Linie 224
Linie 225
Linie 226
Linie 227
Linie 228
Linie 229
Linie 230
Linie 231
Linie 232
Linie 233
Linie 234
Linie 235
Linie 236
Linie 237
Linie 238
Linie 239
Linie 240
Linie 241
Linie 242
Linie 243
Linie 244
Linie 245
Linie 246
Linie 247
Linie 248
Linie 249
Linie 250
Linie 251
Linie 252
Linie 253
Linie 254
Linie 255
Linie 256
Linie 257
Linie 258
Linie 259
Linie 260
Linie 261
Linie 262
Linie 263
Linie 264
Linie 265
Linie 266
Linie 267
Linie 268
Linie 269
Linie 270
Linie 271
Linie 272
Linie 273
Linie 274
Linie 275
Linie 276
Linie 277
Linie 278
Linie 279
Linie 280
Linie 281
Linie 282
Linie 283
Linie 284
Linie 285
Linie 286
Linie 287
Linie 288
Linie 289
Linie 290
Linie 291
Linie 292
Linie 293
Linie 294
Linie 295
Linie 296
Linie 297
Linie 298
Linie 299
Linie 300
Linie 301
Linie 302
Linie 303
Linie 304
Linie 305
Linie 306
Linie 307
Linie 308
Linie 309
Linie 310
Linie 311
Linie 312
Linie 313
Linie 314
Linie 315
Linie 316
Linie 317
Linie 318
Linie 319
Linie 320
Linie 321
Linie 322
Linie 323
Linie 324
Linie 325
Linie 326
Linie 327
Linie 328
Linie 329
Linie 330
Linie 331
Linie 332
Linie 333
Linie 334
Linie 335
Linie 336
Linie 337
Linie 338
Linie 339
Linie 340
Linie 341
Linie 342
Linie 343
Linie 344
Linie 345
Linie 346
Linie 347
Linie 348
Linie 349
Linie 350
Linie 351
Linie 352
Linie 353
Linie 354
Linie 355
Linie 356
Linie 357
Linie 358
Linie 359
Linie 360
Linie 361
Linie 362
Linie 363
Linie 364
Linie 365
Linie 366
Linie 367
Linie 368
Linie 369
Linie 370
Linie 371
Linie 372
Linie 373
Linie 374
Linie 375
Linie 376
Linie 377
Linie 378
Linie 379
Linie 380
Linie 381
Linie 382
Linie 383
Linie 384
Linie 385
Linie 386
Linie 387
Linie 388
Linie 389
Linie 390
Linie 391
Linie 392
Linie 393
Linie 394
Linie 395
Linie 396
Linie 397
Linie 398
Linie 399
Linie 400
Linie 401
Linie 402
Linie 403
Linie 404
Linie 405
Linie 406
Linie 407
Linie 408
Linie 409
Linie 410
Linie 411
Linie 412
Linie 413
Linie 414
Linie 415
Linie 416
Linie 417
Linie 418
Linie 419
Linie 420
Linie 421
Linie 422
Linie 423
Linie 424
Linie 425
Linie 426
Linie 427
Linie 428
Linie 429
Linie 430
Linie 431
Linie 432
Linie 433
Linie 434
Linie 435
Linie 436
Linie 437
Linie 438
Linie 439
Linie 440
Linie 441
Linie 442
Linie 443
Linie 444
Linie 445
Linie 446
Linie 447
Linie 448
Linie 449
Linie 450
Linie 451
Linie 452
Linie 453
Linie 454
Linie 455
Linie 456
Linie 457
Linie 458
Linie 459
Linie 460
Linie 461
Linie 462
Linie 463
Linie 464
Linie 465
Linie 466
Linie 467
Linie 468
Linie 469
Linie 470
Linie 471
Linie 472
Linie 473
Linie 474
Linie 475
Linie 476
Linie 477
Linie 478
Linie 479
Linie 480
Linie 481
Linie 482
Linie 483
Linie 484
Linie 485
Linie 486
Linie 487
Linie 488
Linie 489
Linie 490
Linie 491
Linie 492
Linie 493
Linie 494
Linie 495
Linie 496
Linie 497
Linie 498
Linie 499
Linie 500
Linie 501
Linie 502
Linie 503
Linie 504
Linie 505
Linie 506
Linie 507
Linie 508
Linie 509
Linie 510
Linie 511
Linie 512
Linie 513
Linie 514
Linie 515
Linie 516
Linie 517
Linie 518
Linie 519
Linie 520
Linie 521
Linie 522
Linie 523
Linie 524
Linie 525
Linie 526
Linie 527
Linie 528
Linie 529
Linie 530
Linie 531
Linie 532
Linie 533
Linie 534
Linie 535
Linie 536
Linie 537
Linie 538
Linie 539
Linie 540
Linie 541
Linie 542
Linie 543
Linie 544
Linie 545
Linie 546
Linie 547
Linie 548
Linie 549
Linie 550
Linie 551
Linie 552
Linie 553
Linie 554
Linie 555
Linie 556
Linie 557
Linie 558
Linie 559
Linie 560
Linie 561
Linie 562
Linie 563
Linie 564
Linie 565
Linie 566
Linie 567
Linie 568
Linie 569
Linie 570
Linie 571
Linie 572
Linie 573
Linie 574
Linie 575
Linie 576
Linie 577
Linie 578
Linie 579
Linie 580
Linie 581
Linie 582
Linie 583
Linie 584
Linie 585
Linie 586
Linie 587
Linie 588
Linie 589
Linie 590
Linie 591
Linie 592
Linie 593
Linie 594
Linie 595
Linie 596
Linie 597
Linie 598
Linie 599
Linie 600
Linie 601
Linie 602
Linie 603
Linie 604
Linie 605
Linie 606
Linie 607
Linie 608
Linie 609
Linie 610
Linie 611
Linie 612
Linie 613
Linie 614
Linie 615
Linie 616
Linie 617
Linie 618
Linie 619
Linie 620
Linie 621
Linie 622
Linie 623
Linie 624
Linie 625
Linie 626
Linie 627
Linie 628
Linie 629
Linie 630
Linie 631
Linie 632
Linie 633
Linie 634
Linie 635
Linie 636
Linie 637
Linie 638
Linie 639
Linie 640
Linie 641
Linie 642
Linie 643
Linie 644
Linie 645
Linie 646
Linie 647
Linie 648
Linie 649
Linie 650
Linie 651
Linie 652
Linie 653
Linie 654
Linie 655
Linie 656
Linie 657
Linie 658
Linie 659
Linie 660
Linie 661
Linie 662
Linie 663
Linie 664
Linie 665
Linie 666
Linie 667
Linie 668
Linie 669
Linie 670
Linie 671
Linie 672
Linie 673
Linie 674
Linie 675
Linie 676
Linie 677
Linie 678
Linie 679
Linie 680
Linie 681
Linie 682
Linie 683
Linie 684
Linie 685
Linie 686
Linie 687
Linie 688
Linie 689
Linie 690
Linie 691
Linie 692
Linie 693
Linie 694
Linie 695
Linie 696
Linie 697
Linie 698
Linie 699
Linie 700
Linie 701
Linie 702
Linie 703
Linie 704
Linie 705
Linie 706
Linie 707
Linie 708
Linie 709
Linie 710
Linie 711
Linie 712
Linie 713
Linie 714
Linie 715
Linie 716
Linie 717
Linie 718
Linie 719
Linie 720
Linie 721
Linie 722
Linie 723
Linie 724
Linie 725
Linie 726
Linie 727
Linie 728
Linie 729
Linie 730
Linie 731
Linie 732
Linie 733
Linie 734
Linie 735
Linie 736
Linie 737
Linie 738
Linie 739
Linie 740
Linie 741
Linie 742
Linie 743
Linie 744
Linie 745
Linie 746
Linie 747
Linie 748
Linie 749
Linie 750
Linie 751
Linie 752
Linie 753
Linie 754
Linie 755
Linie 756
Linie 757
Linie 758
Linie 759
Linie 760
Linie 761
Linie 762
Linie 763
Linie 764
Linie 765
Linie 766
Linie 767
Linie 768
Linie 769
Linie 770
Linie 771
Linie 772
Linie 773
Linie 774
Linie 775
Linie 776
Linie 777
Linie 778
Linie 779
Linie 780
Linie 781
Linie 782
Linie 783
Linie 784
Linie 785
Linie 786
Linie 787
Linie 788
Linie 789
Linie 790
Linie 791
Linie 792
Linie 793
Linie 794
Linie 795
Linie 796
Linie 797
Linie 798
Linie 799
Linie 800
Linie 801
Linie 802
Linie 803
Linie 804
Linie 805
Linie 806
Linie 807
Linie 808
Linie 809
Linie 810
Linie 811
Linie 812
Linie 813
Linie 814
Linie 815
Linie 816
Linie 817
Linie 818
Linie 819
Linie 820
Linie 821
Linie 822
Linie 823
Linie 824
Linie 825
Linie 826
Linie 827
Linie 828
Linie 829
Linie 830
Linie 831
Linie 832
Linie 833
Linie 834
Linie 835
Linie 836
Linie 837
Linie 838
Linie 839
Linie 840
Linie 841
Linie 842
Linie 843
Linie 844
Linie 845
Linie 846
Linie 847
Linie 848
Linie 849
Linie 850
Linie 851
Linie 852
Linie 853
Linie 854
Linie 855
Linie 856
Linie 857
Linie 858
Linie 859
Linie 860
Linie 861
Linie 862
Linie 863
Linie 864
Linie 865
Linie 866
Linie 867
Linie 868
Linie 869
Linie 870
Linie 871
Linie 872
Linie 873
Linie 874
Linie 875
Linie 876
Linie 877
Linie 878
Linie 879
Linie 880
Linie 881
Linie 882
Linie 883
Linie 884
Linie 885
Linie 886
Linie 887
Linie 888
Linie 889
Linie 890
Linie 891
Linie 892
Linie 893
Linie 894
Linie 895
Linie 896
Linie 897
Linie 898
Linie 899
Linie 900
Linie 901
Linie 902
Linie 903
Linie 904
Linie 905
Linie 906
Linie 907
Linie 908
Linie 909
Linie 910
Linie 911
Linie 912
Linie 913
Linie 914
Linie 915
Linie 916
Linie 917
Linie 918
Linie 919
Linie 920
Linie 921
Linie 922
Linie 923
Linie 924
Linie 925
Linie 926
Linie 927
Linie 928
Linie 929
Linie 930
Linie 931
Linie 932
Linie 933
Linie 934
Linie 935
Linie 936
Linie 937
Linie 938
Linie 939
Linie 940
Linie 941
Linie 942
Linie 943
Linie 944
Linie 945
Linie 946
Linie 947
Linie 948
Linie 949
Linie 950
Linie 951
Linie 952
Linie 953
Linie 954
Linie 955
Linie 956
Linie 957
Linie 958
Linie 959
Linie 960
Linie 961
Linie 962
Linie 963
Linie 964
Linie 965
Linie 966
Linie 967
Linie 968
Linie 969
Linie 970
Linie 971
Linie 972
Linie 973
Linie 974
Linie 975
Linie 976
Linie 977
Linie 978
Linie 979
Linie 980
Linie 981
Linie 982
Linie 983
Linie 984
Linie 985
Linie 986
Linie 987
Linie 988
Linie 989
Linie 990
Linie 991
Linie 992
Linie 993
Linie 994
Linie 995
Linie 996
Linie 997
Linie 998
Linie 999
Linie 1000

Durchgehende Verbindung mit der Buslinie 3

Anreise vom Hauptbahnhof zum

1. **JUFA Gästehaus (Ausstieg Haltestelle Justizgebäude oder Akademiestrasse),**
2. **Naturwissenschaftliche Fakultät, Hellbrunner Str. 34 (Ausstieg Haltestelle Faistauergasse oder Josefiau) und**
3. **Motel One (Ausstieg Haltestelle Polizeidirektion)**

3 Itzling Pflanzmann - Hauptbahnhof - Zentrum - Alpenstraße - Salzburg Süd

Fahrplan 2012 - gültig ab 11.12.2011 bis 08.12.2012

Montag bis Freitag

Stunde		4	5	6	7	8-18	19	20	21	22	23	0
Verkehrsbeschränkung											MD FF MD FF	FF
Hinweise											nAi nAi	nAi
Itzling Pflanzmann	ab		38 58	08 18 28 38 46 56	06 16 26 36 46 56	06 16 26 36 46 56	06 18 28 38 48 58	18 38 58	18 38 58	18 38 58	01 18 31 38	01
Zweigstraße			39 59	09 19 29 39 48 58	08 18 28 38 48 58	08 18 28 38 48 58	08 19 29 39 49 59	19 39 59	19 39 59	19 39 59	02 19 32 39	02
Goethestraße			41 01	11 21 31 41 49 59	09 19 29 39 49 59	09 19 29 39 49 59	09 21 31 41 51 01	21 41	01 21 41	01 21 41	03 21 33 41	03
Kirchenstraße HTL Itzling			42 02	12 22 32 42 51 01	11 21 31 41 51 01	11 21 31 41 51 01	11 22 32 42 52 02	22 42	02 22 42	02 22 42	04 22 34 42	04
Werkstättenstraße			43 03	13 23 33 43 52 02	12 22 32 42 52 02	12 22 32 42 52 02	12 23 33 43 53 03	23 43	03 23 43	03 23 43	04 23 34 43	04
August Gruber Straße			44 04	14 24 34 44 53 03	13 23 33 43 53 03	13 23 33 43 53 03	13 24 34 44 54 04	24 44	04 24 44	04 24 44	05 24 35 44	05
Engelbert Weiß Weg			45 05	15 25 35 45 54 04	14 24 34 44 54 04	14 24 34 44 54 04	14 25 35 45 55 05	25 45	05 25 45	05 25 45	06 25 36 45	06
Hauptbahnhof (Busleiste C)		15 57	16 46	06 16 26 36 46 56	06 16 26 36 46 56	06 16 26 36 46 56	06 16 26 36 46 56	06 26 46	06 26 46	06 26 46	06 08 26 38 46	08
Kiesel		17 59	18 48	08 18 28 38 48 58	08 18 28 38 48 58	08 18 28 38 48 58	08 18 28 38 48 58	08 28 48	08 28 48	08 28 48	08 09 28 39 48	09
Kongreßhaus		18 00	20 50	10 20 30 40 50 59	09 19 29 39 49 59	09 19 29 39 49 59	09 19 30 40 50 00	10 30 50	10 30 50	10 30 50	10 11 30 41 50	11
Mirabellplatz (Mozarteum)		19 01	21 51	11 21 31 41 51 01	11 21 31 41 51 01	11 21 31 41 51 01	11 21 31 41 51 01	11 31 51	11 31 51	11 31 51	11 12 31 42 51	12
Makartplatz (Theater)		20 03	22 52	12 22 32 42 52 02	12 22 32 42 52 02	12 22 32 42 52 02	12 22 32 42 52 02	12 32 52	12 32 52	12 32 52	12 13 32 43 52	13
Rathaus		22 05	24 54	14 24 34 44 54 05	15 25 35 45 55 05	15 25 35 45 55 05	15 25 34 44 54 04	14 34 54	14 34 54	14 34 54	14 15 34 45 54	15
Mozartsteg/Rudolfskai		24 06	26 56	16 26 36 46 56 06	16 26 36 46 56 06	16 26 36 46 56 06	16 26 36 46 56 06	16 36 56	16 36 56	16 36 56	16 17 36 47 56	17
Justizgebäude		25 08	27 57	17 27 37 47 57 08	18 28 38 48 58 08	18 28 38 48 58 08	18 28 37 47 57 07	17 37 57	17 37 57	17 37 57	17 18 37 48 57	18
Akademiestraße		26 09	28 58	18 28 38 48 58 09	19 29 39 49 59 09	19 29 39 49 59 09	19 29 38 48 58 08	18 38 58	18 38 58	18 38 58	18 18 38 48 58	18
Faistauergasse		27 10	29 59	19 29 39 49 59 10	20 30 40 50 00 10	20 30 40 50 00 10	20 30 39 49 59 09	19 39 59	19 39 59	19 39 59	19 19 39 49 59	19
Josefiau		28 11	31 01	21 31 41 51 01 12	22 32 42 52 02 12	22 32 42 52 02 12	22 32 41 51 01 11	21 41	01 21 41	01 21 41	01 21 20 41 50	01 20
Hermau		29 12	32 02	22 32 42 52 02 13	23 33 43 53 03 13	23 33 43 53 03 13	23 33 42 52 02	12 22 42	02 22 42	02 22 42	02 22 21 42 51	02 21
Polizeidirektion		29 14	33 03	23 33 43 53 03 15	25 35 45 55 05 15	25 35 45 55 05 15	25 35 43 53 03 13	23 43	03 23 43	03 23 43	03 23 22 43 52	03 22
Ginzkeyplatz		30 15	34 04	24 34 44 54 04 17	27 37 47 57 07 17	27 37 47 57 07 17	27 37 44 54 04	14 24 44	04 24 44	04 24 44	04 24 23 53	23
P+R Alpensiedlung		32 16	36 06	26 36 46 56 06 19	29 39 49 59 09 19	29 39 49 59 09 19	29 39 46 56 06	16 26 46	06 26 46	06 26 46	06 26 24 54	24
Salzburg Süd S-Bahn	an	33 17	37 07	27 37 47 57 07	20 30 40 50 00	10 20 30 40 50 00	10 20 30 40 47 57	07 17 27 47	07 27 47	07 27 47	07 27	
Salzburg Süd Kaindlweberweg	an										25 55	25

Salzburg AG - StadtBus, Plainstraße 70, 5020 Salzburg, Tel. +43 (0)662 44 801 500

Montag bis Freitag

Stunde		0	1
Verkehrsbeschränkung		MD FF	FF
Hinweise			
Itzling Pflanzmann	ab	31	01
Zweigstraße		32	02
Goethestraße		33	03
Kirchenstraße HTL Itzling		34	04
Werkstättenstraße		34	04
August Gruber Straße		35	05
Engelbert Weiß Weg		06 36	06
Hauptbahnhof (Busleiste C)		08 38	08
Kiesel		09 39	09
Kongreßhaus		11 41	11
Mirabellplatz (Mozarteum)		12 42	12
Makartplatz (Theater)		13 43	13
Rathaus		15 45	15
Mozartsteg/Rudolfskai		17 47	17
Justizgebäude		18 48	18
Akademiestraße		18 48	18
Faistauergasse		19 49	19
Josefiau		20 50	20
Hermau		21 51	21
Polizeidirektion		22 52	22
Ginzkeyplatz		53	23
P+R Alpensiedlung		54	24
Salzburg Süd S-Bahn	an	55	25
Salzburg Süd Kaindlweberweg	an		

Salzburg AG - StadtBus, Plainstraße 70, 5020 Salzburg, Tel. +43 (0)662 44 801 500

Samstag

Stunde		4	5	6	7	8	9-17	18	19-21	22	23	0	1
Verkehrsbeschränkung													
Hinweise											nAi nAi	nAi	
Itzling Pflanzmann	ab		58	18 38 58	18 38 58	08 18 26 36 46 56	06 16 26 36 46 56	08 18 28 38 58	18 38 58	18 38	01 31 38	01 31	01
Zweigstraße			59	19 39 59	19 39 59	09 19 28 38 48 58	08 18 28 38 48 58	09 19 29 39 59	19 39 59	19 39	02 32 39	02 32	02
Goethestraße			01	21 41 01	21 41 01	11 21 29 39 49 59	09 19 29 39 49 59	11 21 31 41 01	21 41 01	21 41	03 33 41	03 33	03
Kirchenstraße HTL Itzling			02	22 42 02	22 42 02	12 22 31 41 51 01	11 21 31 41 51 01	12 22 32 42 02	22 42 02	22 42	04 34 42	04 34	04
Werkstättenstraße			03	23 43 03	23 43 03	13 23 32 42 52 02	12 22 32 42 52 02	13 23 33 43 03	23 43 03	23 43	04 34 43	04 34	04
August Gruber Straße			04	24 44 04	24 44 04	14 24 33 43 53 03	13 23 33 43 53 03	14 24 34 44 04	24 44 04	24 44	05 35 44	05 35	05
Engelbert Weiß Weg			05	25 45 05	25 45 05	15 25 34 44 54 04	14 24 34 44 54 04	15 25 35 45 05	25 45 05	25 45	06 36 45	06 36	06
Hauptbahnhof (Busleiste C)		40	21 06	26 46 06	26 46 06	16 26 36 46 56 06	16 26 36 46 56 06	16 26 36 46 06	26 46 06	26 46	06 38 46	08 38	08
Kiesel		41	23 08	28 48 08	28 48 08	18 28 38 48 58 08	18 28 38 48 58 08	18 28 38 48 08	28 48 08	28 48	09 39 48	09 39	09
Kongreßhaus		43	24 10	30 50 10	30 50 10	20 30 39 49 59 09	19 29 39 49 59 09	20 30 40 50 10	30 50 10	30 50	11 41 50	11 41	11
Mirabellplatz (Mozarteum)		44	25 11	31 51 11	31 51 11	21 31 41 51 01	11 21 31 41 51 01	21 31 41 51 11	31 51 11	31 51	12 42 51	12 42	12
Makartplatz (Theater)		45	27 12	32 52 12	32 52 12	22 32 42 52 02	12 22 32 42 52 02	22 32 42 52 12	32 52 12	32 52	13 43 52	13 43	13
Rathaus		47	29 14	34 54 14	34 54 14	24 34 45 55 05	15 25 35 45 55 05	24 34 44 54 14	34 54 14	34 54	15 45 54	15 45	15
Mozartsteg/Rudolfskai		49	30 16	36 56 16	36 56 16	26 36 46 56 06	16 26 36 46 56 06	26 36 46 56 16	36 56 16	36 56	17 47 56	17 47	17
Justizgebäude		50	32 17	37 57 17	37 57 17	27 37 48 58 08	18 28 38 48 58 08	27 37 47 57 17	37 57 17	37 57	18 48 57	18 48	18
Akademiestraße		50	33 18	38 58 18	38 58 18	28 38 49 59 09	19 29 39 49 59 09	28 38 48 58 18	38 58 18	38 58	18 48 58	18 48	18
Faistauergasse		51	34 19	39 59 19	39 59 19	29 39 50 00 10	20 30 40 50 00 10	29 39 49 59 19	39 59 19	39 59	19 49 59	19 49	19
Josefiau		52	35 21	41 01 21	41 01 21	31 41 52 02 12	22 32 42 52 02 12	31 41 51 01 21	41 01 21	41 01	20 50 01	20 50	20
Hermau		53	36 22	42 02 22	42 02 22	32 42 53 03 13	23 33 43 53 03 13	32 42 52 02 22	42 02 22	42 02	21 51 02	21 51	21
Polizeidirektion		54	38 23	43 03 23	43 03 23	33 43 55 05 15	25 35 45 55 05 15	33 43 53 03 23	43 03 23	43 03	22 52 03	22 52	22
Ginzkeyplatz		55	39 24	44 04 24	44 04 24	34 44 56 06 16	26 36 46 56 06 16	34 44 54 04 24	44 04 24	44 04	23 53	23 53	23
P+R Alpensiedlung		56	40 26	46 06 26	46 06 26	36 46 58 08 18	28 38 48 58 08 18	36 46 56 06 26	46 06 26	46 06	24 54	24 54	24
Salzburg Süd S-Bahn	an	57	41 27	47 07 27	47 07 27	37 47 59 09 19	29 39 49 59 09 19	37 47 57 07 27	47 07 27	47 07		55	25
Salzburg Süd Kaindlweberweg	an										25 55	25	

Salzburg AG - StadtBus, Plainstraße 70, 5020 Salzburg, Tel. +43 (0)662 44 801 500

FF = verkehrt Freitag und vor Feiertag MD = Montag - Donnerstag (Werktag), nicht vor Feiertag nAi = bis P+R Alpensiedlung, dann weiter als Linie 7 Richtung Aigen

Bitte Sonderfahrpläne am Heiligen Abend, zu Silvester und Mariä Empfängnis beachten.

003/2012/1/1

Durchgehende Verbindung mit der Buslinie 3

Abreise vom
1. Motel One (Einstieg Haltestelle Polizeidirektion)
2. Naturwissenschaftliche Fakultät (Einstieg Haltestelle Josefiau oder Faistauergasse)
3. JUFA Gästehaus (Einstieg Haltestelle Akademiestraße oder Justizgebäude)

zum Hauptbahnhof:

3 Salzburg Süd - Alpenstraße - Zentrum - Hauptbahnhof - Itzling Pflanzmann

Fahrplan 2012 - gültig ab 11.12.2011 bis 08.12.2012

Montag bis Freitag

Stunde		3	4	5	6	7-18	19	20-22	23		0	1
Verkehrsbeschränkung									FF	MD FF	FF	FF
Hinweise												
Salzburg Süd Kaindlweberweg	ab								29	59	29	
Salzburg Süd S-Bahn	ab		36	20 30 40	00 10 20 30 40 50	00 10 20 30 40 50	00 10 20 40	00 20 40	00			28
P+R Alpensiedlung			38	22 32 42	02 13 23 33 43 53	03 13 23 33 43 53	02 12 22 42	02 22 42	02 30	00	30	30
Ginzkeyplatz			39	24 34 44	04 15 25 35 45 55	05 15 25 35 45 55	04 14 24 44	04 24 44	04 31	01	31	31
Polizeidirektion		43	40	05 25 35 45 55	05 16 26 36 46 56	06 16 26 36 46 56	05 15 25 45	05 25 45	05 32 41	02	32	32
Herrnau		44	41	06 26 36 46 56	06 18 28 38 48 58	08 18 28 38 48 58	06 16 26 46	06 26 46	06 33 42	03	33	33
Josefiau		45	42	08 28 38 48 58	08 19 29 39 49 59	09 19 29 39 49 59	08 18 28 48	08 28 48	08 35 44	05	35	35
Faistauergasse		46	43	09 29 39 49 59	09 21 31 41 51	01 11 21 31 41 51	09 19 29 49	09 29 49	09 36 45	06	36	36
Akademiestraße		48	45	11 31 41 51	01 11 22 32 42 52	02 12 22 32 42 52	02 11 21 31 51	11 31 51	11 38 47	08	38	38
Justizgebäude		49	46	12 32 42 52	02 12 24 34 44 54	04 14 24 34 44 54	04 12 22 32 52	12 32 52	12 39 48	09	39	39
Äußerer Stein		51	48	15 35 45 55	05 15 27 37 47 57	07 17 27 37 47 57	07 15 25 35 55	15 35 55	15 42 50	12	42	42
Mozartsteg/Imbergstraße			49	16 36 46 56	06 16 28 38 48 58	08 18 28 38 48 58	08 16 26 36 56	16 36 56	16 43 51	13	43	43
Theatergasse			50	18 38 48 58	08 18 30 40 50	00 10 20 30 40 50	00 10 18 28 38 58	18 38 58	18 45 53	15	45	45
Mirabellplatz (Andrä-Kirche 7)			51	20 40 50	00 10 20 32 42 52	02 12 22 32 42 52	02 12 20 30 40	00 20 40	00 20 46	55	16	46
Kongreßhaus			52	21 41 51	01 11 21 33 43 53	03 13 23 33 43 53	03 13 21 31 41	01 21 41	01 21 47	56	17	47
Kiesel			53	21 41 51	01 11 21 34 44 54	04 14 24 34 44 54	04 14 21 31 41	01 21 41	01 21 48	56	18	48
Hauptbahnhof (Busleiste D)			55	24 44 54	04 14 24 37 47 57	07 17 27 37 47 57	07 17 24 34 44	04 24 44	04 24 51	59	21	51
Engelbert Weiß Weg				25 45 55	05 15 25 38 48 58	08 18 28 38 48 58	08 18 25 35 45	05 25 45	05 25 51		21	51
August Gruber Straße				25 45 55	05 15 25 39 49 59	09 19 29 39 49 59	09 19 25 35 45	05 25 45	05 25 52		22	52
Werkstättenstraße				26 46 56	06 16 26 40 50	00 10 20 30 40 50	00 10 20 26 36 46	06 26 46	06 26 53		23	53
Kirchenstraße HTL Itzling				27 47 57	07 17 27 41 51	01 11 21 31 41 51	01 11 21 27 37 47	07 27 47	07 27 53		23	53
Goethestraße				28 48 58	08 18 28 42 52	02 12 22 32 42 52	02 12 22 28 38 48	08 28 48	08 28 54		24	54
Zweigstraße				29 49 59	09 19 29 43 53	03 13 23 33 43 53	03 13 23 29 39 49	09 29 49	09 29 55		25	55
Itzling Pflanzmann	an			30 50 00	10 20 30 44 54	04 14 24 30 40 50	10 30 50	10 30 50	10 30 55		25	55

Salzburg AG - StadtBus, Plainstraße 70, 5020 Salzburg, Tel. +43 (0)662 44 801 500

Samstag

Stunde		4	5	6	7	8	9-17	18	19-22	23	0	1
Verkehrsbeschränkung												
Hinweise												
Salzburg Süd Kaindlweberweg	ab									29 59	29	
Salzburg Süd S-Bahn	ab		00 20 40	00 20 40	00 20 40	00 20 30 40 50	00 10 20 30 40 50	00 20 40	00 20 40	00		28
P+R Alpensiedlung			02 22 42	02 22 42	02 22 42	02 23 33 43 53	03 13 23 33 43 53	03 22 42	02 22 42	02 30	00 30	30
Ginzkeyplatz			03 24 44	04 24 44	04 24 44	04 25 35 45 55	05 15 25 35 45 55	05 24 44	04 24 44	04 31	01 31	31
Polizeidirektion		07	04 25 45	05 25 45	05 25 35 45 55	05 15 26 36 46 56	06 16 26 36 46 56	06 25 45	05 25 45	05 32	02 32	32
Herrnau		08	05 26 46	06 26 46	06 26 36 46 56	06 16 28 38 48 58	08 18 28 38 48 58	08 26 46	06 26 46	06 33	03 33	33
Josefiau		10	06 28 48	08 28 48	08 28 38 48 58	08 18 29 39 49 59	09 19 29 39 49 59	09 28 48	08 28 48	08 35	05 35	35
Faistauergasse		11	07 29 49	09 29 49	09 29 39 49 59	09 19 31 41 51	01 11 21 31 41 51	01 29 49	09 29 49	09 36	06 36	36
Akademiestraße		12	09 31 51	11 31 51	11 31 41 51	01 11 21 32 42 52	02 12 22 32 42 52	02 12 31 51	11 31 51	11 38	08 38	38
Justizgebäude		13	10 32 52	12 32 52	12 32 42 52	02 12 22 34 44 54	04 14 24 34 44 54	04 14 32 52	12 32 52	12 39	09 39	39
Äußerer Stein		15	12 35 55	15 35 55	15 35 45 55	05 15 25 37 47 57	07 17 27 37 47 57	07 17 35 55	15 35 55	15 42	12 42	42
Mozartsteg/Imbergstraße			13 36 56	16 36 56	16 36 46 56	06 16 26 38 48 58	08 18 28 38 48 58	08 18 36 56	16 36 56	16 43	13 43	43
Theatergasse			14 38 58	18 38 58	18 38 48 58	08 18 28 40 50	00 10 20 30 40 50	00 10 20 38 58	18 38 58	18 45	15 45	45
Mirabellplatz (Andrä-Kirche 7)			15 40 00	20 40 00	20 40 50 00	10 20 30 42 52	02 12 22 32 42 52	02 12 22 40 00	20 40 00	20 46	16 46	46
Kongreßhaus			16 41 01	21 41 01	21 41 51 01	11 21 31 43 53	03 13 23 33 43 53	03 13 23 41 01	21 41 01	21 47	17 47	47
Kiesel			17 41 01	21 41 01	21 41 51 01	11 21 31 44 54	04 14 24 34 44 54	04 14 24 41 01	21 41 01	21 48	18 48	48
Hauptbahnhof (Busleiste D)			19 44 04	24 44 04	24 44 54 04	14 24 34 47 57	07 17 27 37 47 57	07 17 27 44 04	24 44 04	24 51	21 51	50
Engelbert Weiß Weg			45 05	25 45 05	25 45 55 05	15 25 35 48 58	08 18 28 38 48 58	08 18 28 45 05	25 45 05	25 51	21 51	
August Gruber Straße			45 05	25 45 05	25 45 55 05	15 25 35 49 59	09 19 29 39 49 59	09 19 29 45 05	25 45 05	25 52	22 52	
Werkstättenstraße			46 06	26 46 06	26 46 56 06	16 26 36 50 00	10 20 30 40 50 00	10 20 30 46 06	26 46 06	26 53	23 53	
Kirchenstraße HTL Itzling			47 07	27 47 07	27 47 57 07	17 27 37 51 01	11 21 31 41 51 01	11 21 31 47 07	27 47 07	27 53	23 53	
Goethestraße			48 08	28 48 08	28 48 58 08	18 28 38 52 02	12 22 32 42 52 02	12 22 32 48 08	28 48 08	28 54	24 54	
Zweigstraße			49 09	29 49 09	29 49 59 09	19 29 39 53 03	13 23 33 43 53 03	13 23 33 49 09	29 49 09	29 55	25 55	
Itzling Pflanzmann	an		50 10	30 50 10	30 50 00 10	20 30 40 54 04	14 24 34 44 54 04	14 24 34 50 10	30 50 10	30 55	25 55	

Salzburg AG - StadtBus, Plainstraße 70, 5020 Salzburg, Tel. +43 (0)662 44 801 500

Sonntag und Feiertag

Stunde		4	5	6-8	9	10-22	23		0	1
Verkehrsbeschränkung							VF	NF VF	VF	VF
Hinweise										
Salzburg Süd Kaindlweberweg	ab						29	59	29	
Salzburg Süd S-Bahn	ab		00 58	28 58	20 40	00 20 40	00			28
P+R Alpensiedlung			02	00 30	00 22 42	02 22 42	02 30	00	30	30
Ginzkeyplatz			03	01 31	01 24 44	04 24 44	04 31	01	31	31
Polizeidirektion		07	04 33	02 32	02 25 45	05 25 45	05 32 41	02	32	32
Herrnau		08	05 34	03 33	03 26 46	06 26 46	06 33 42	03	33	33
Josefiau		10	06 35	05 35	05 28 48	08 28 48	08 35 44	05	35	35
Faistauergasse		11	07 36	06 36	06 29 49	09 29 49	09 36 45	06	36	36
Akademiestraße		12	09 38	08 38	08 31 51	11 31 51	11 38 47	08	38	38
Justizgebäude		13	10 39	09 39	09 32 52	12 32 52	12 39 48	09	39	39
Äußerer Stein		15	12 42	12 42	12 35 55	15 35 55	15 42 50	12	42	42
Mozartsteg/Imbergstraße			13 43	13 43	13 36 56	16 36 56	16 43 51	13	43	43
Theatergasse			14 44	14 44	14 38 58	18 38 58	18 45 53	15	45	45
Mirabellplatz (Andrä-Kirche 7)			15 45	15 45	15 40 00	20 40 00	20 46 55	16	46	46
Kongreßhaus			16 46	16 46	16 41 01	21 41 01	21 47 56	17	47	47
Kiesel			17 47	17 47	17 41 01	21 41 01	21 48 56	18	48	48
Hauptbahnhof (Busleiste D)			19 50	20 50	20 44 04	24 44 04	24 51 59	21	51	50
Engelbert Weiß Weg			50	20 50	20 45 05	25 45 05	25 51	21	51	
August Gruber Straße			51	21 51	21 45 05	25 45 05	25 52	22	52	
Werkstättenstraße			52	22 52	22 46 06	26 46 06	26 53	23	53	
Kirchenstraße HTL Itzling			52	22 52	22 47 07	27 47 07	27 53	23	53	
Goethestraße			53	23 53	23 48 08	28 48 08	28 54	24	54	
Zweigstraße			54	24 54	24 49 09	29 49 09	29 55	25	55	
Itzling Pflanzmann	an		54	24 54	24 50 10	30 50 10	30 55	25	55	

Salzburg AG - StadtBus, Plainstraße 70, 5020 Salzburg, Tel. +43 (0)662 44 801 500

FF = verkehrt Freitag und vor Feiertag MD = Montag - Donnerstag (Werktag), nicht vor Feiertag VF = vor Feiertag NF = nicht vor Feiertag

Bitte Sonderfahrpläne am Heiligen Abend, zu Silvester und Mariä Empfängnis beachten.

003/2012/1/1

Bushaltestellen JUFA Gästehaus (A) und NAWI (Zugang über Haupteingang)
Blau: Busroute (nur ab Haltestelle Justizgebäude eingezeichnet)
Grün: Fußweg ab Haltestelle Justizgebäude zu JUFA Gästehaus (A)
vom JUFA Gästehaus (A) zur NAWI Haupteingang (1,4 km ; ca. 15 min)
Fußweg ab Haltestelle Faistauergasse zur NAWI (Haupteingang)

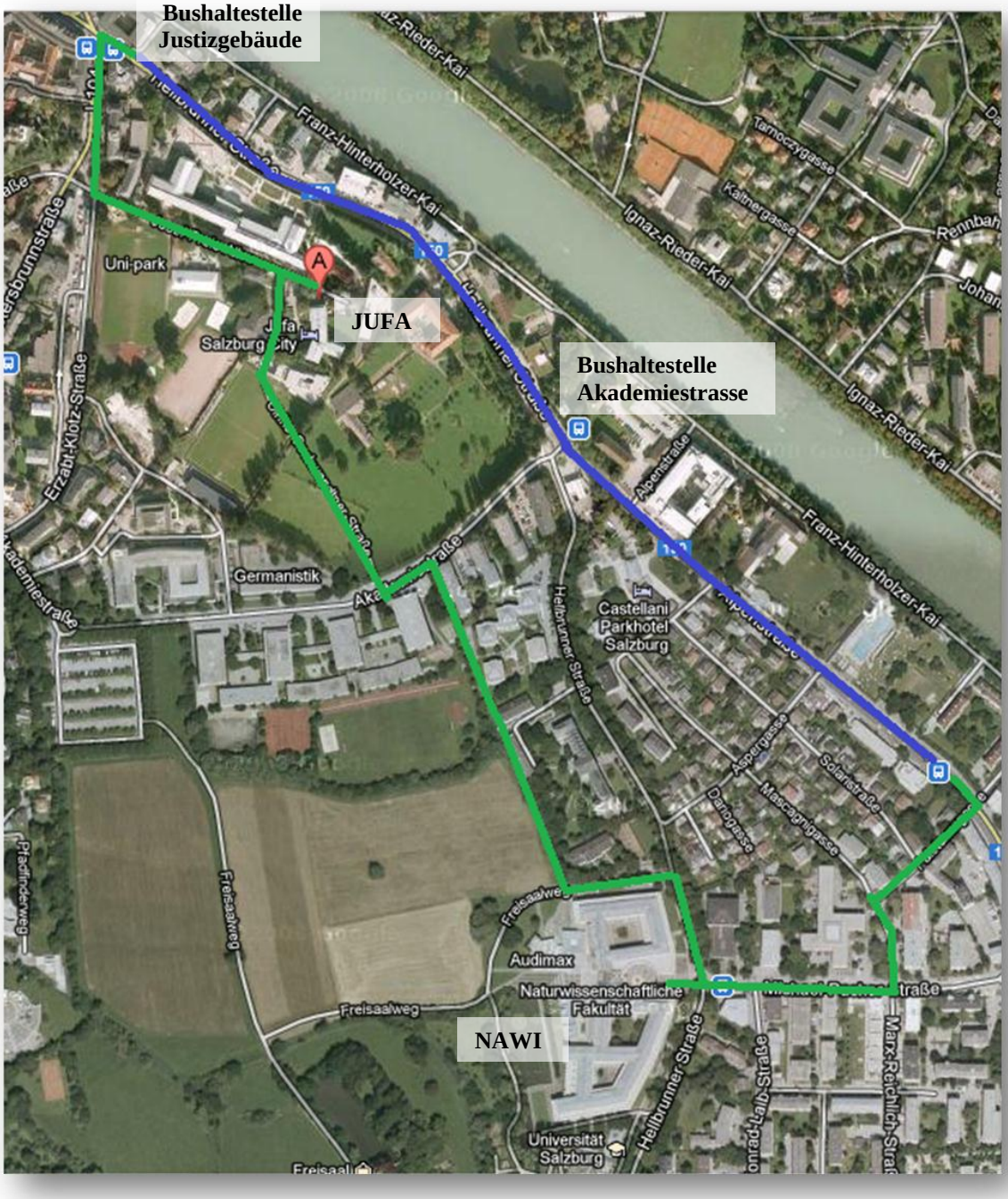

Fußweg: Bushaltstelle Linie 3 Akademiestraße (A) – JUFA Gästehaus (B) (650 m; ca. 8 min)

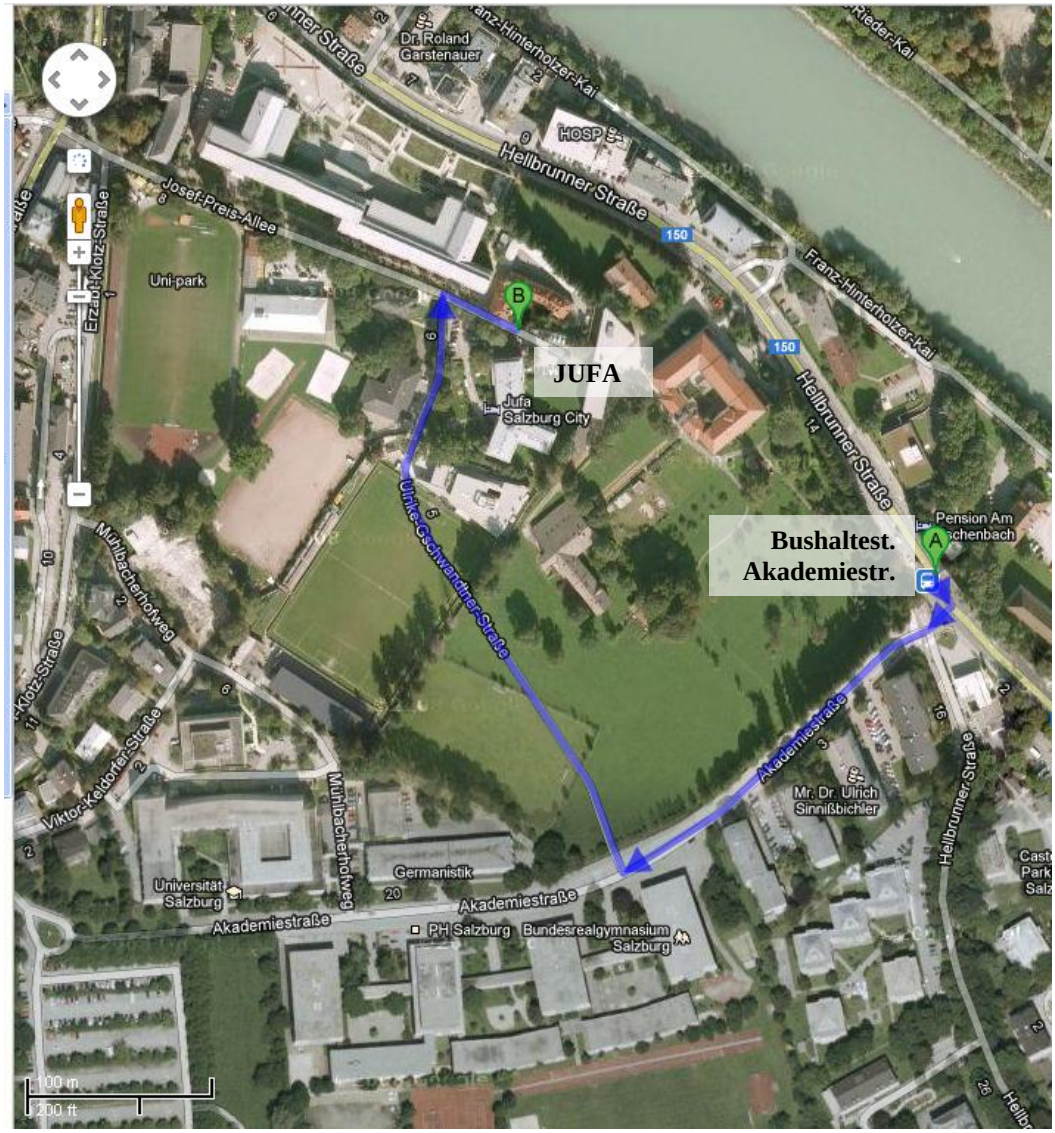

Route: Motel One (A)– NAWI:
Blau: Busroute Haltestelle Polizeidirektion bis Haltestelle Josefiau
Grün: Fußweg von Bushaltestelle zur NAWI oder Fußweg von Motel One über Hellbrunner Allee zur NAWI (1,6 km, ca. 25 min)

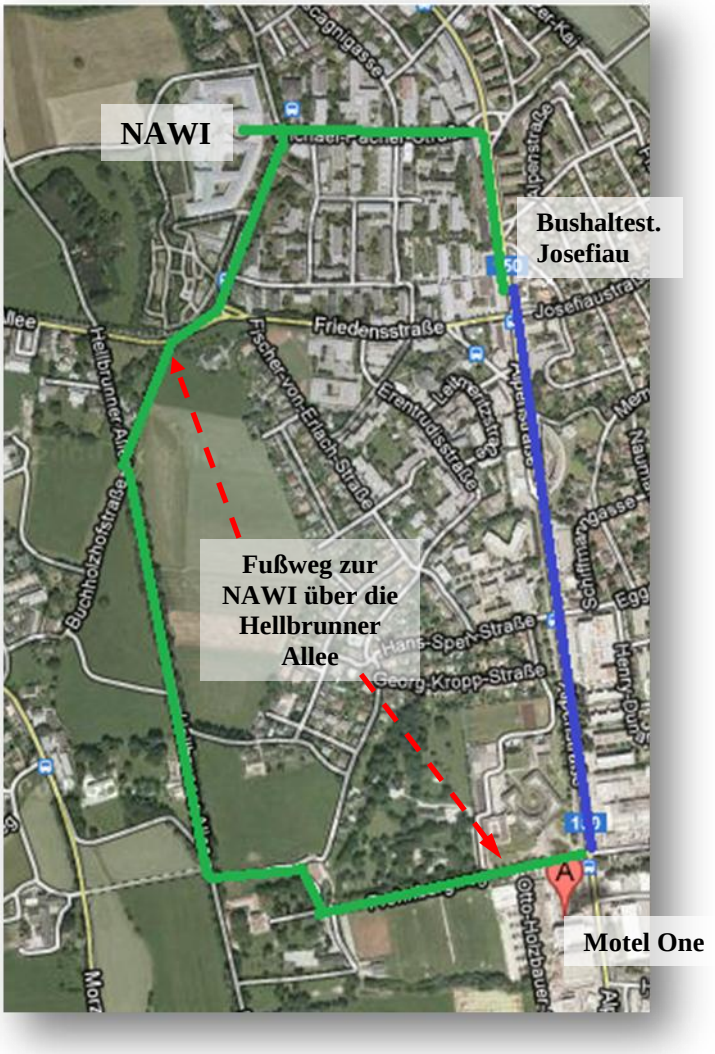

www.wegweiser.ac.at

Lageplan: Grüner HS (HS 403), Uni Salzburg,

A-5020 Salzburg, Hellbrunnerstraße 34, Naturwissenschaften, Erdgeschoß

Übersichtsplan: Uni Salzburg, Areal Nonntal

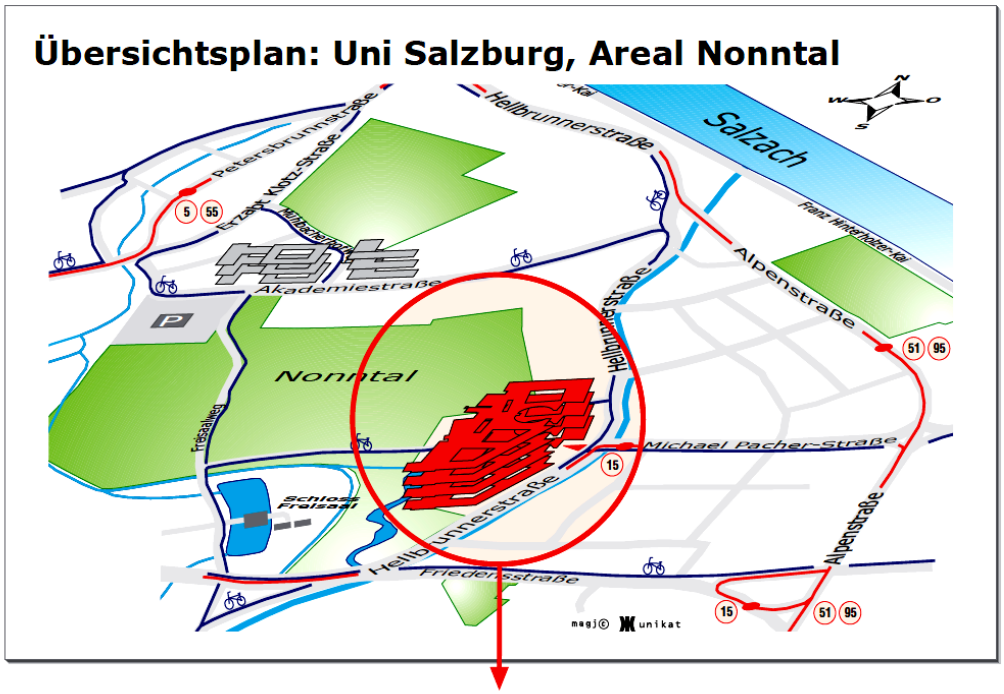

Detailplan: Naturwissenschaften

Erdgeschoß

Grüner HS (HS 403)

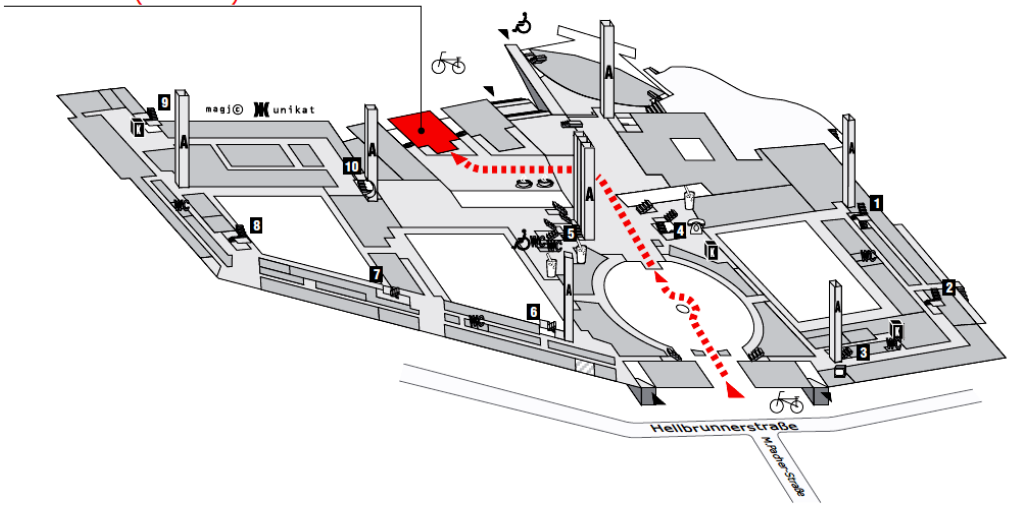

Symbollegende siehe unter www.wegweiser.ac.at/symbollegende.html

Abendveranstaltung am Freitag 1. Juni: Sternbräu, Griesgasse 23–25, 5020 Salzburg
Reservierung in der Kaiserstube ab 20:30

Blaue Route: Motel One (A) – Sternbräu (B) mit Bus:

1. Mit Linie 3 oder 8 von der Haltestelle „Polizeidirektion“ vor dem Motel One stadteinwärts bis Haltestelle „Äußerer Stein“ dort umsteigen
2. Umsteigen in Linie 7 oder 10: von Haltestelle „Äußerer Stein“ bis Haltestelle „Hanuschplatz/Zentrum“, dort aussteigen.
3. ca. 3 min Fußweg zum Sternbräu auf der anderen Straßenseite

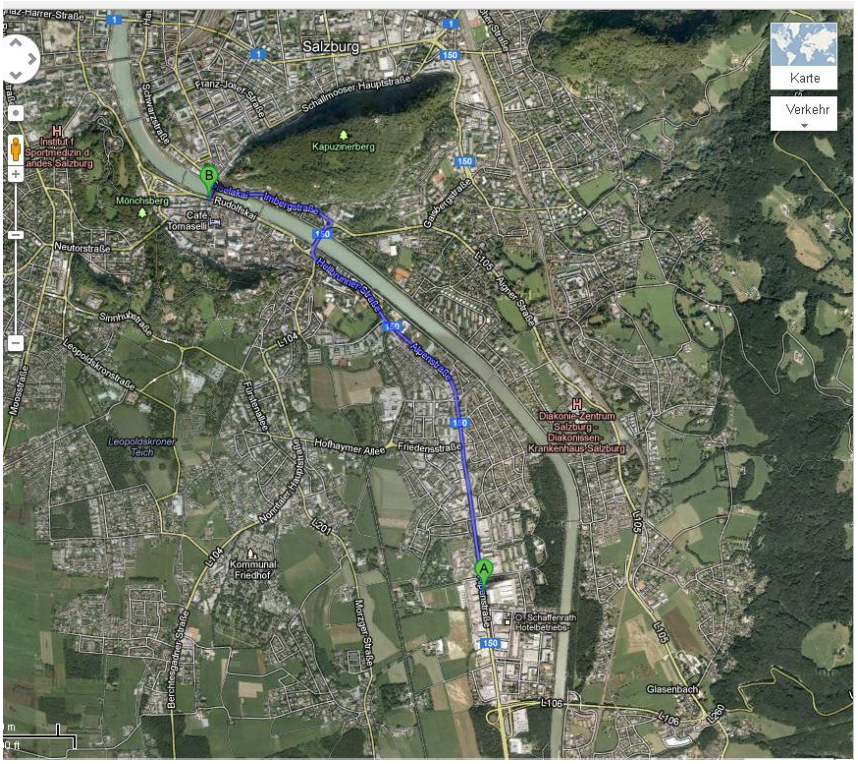

Fußweg von Haltestelle Hanuschplatz/Zentrum zum Sternbräu (B):